cmgh
CELLULAR AND MOLECULAR GASTROENTEROLOGY AND HEPATOLOGY

ORIGINAL RESEARCH

The Critical and Diverse Roles of CD4⁻CD8⁻ Double Negative T Cells in Nonalcoholic Fatty Liver Disease

Changying Li,[1,2,3,4,5,*] Xiaonan Du,[1,2,3,4,5,*] Zongshan Shen,[2,6] Yunxiong Wei,[1,2,3,4,5] Yaning Wang,[1,2,3,4,5] Xiaotong Han,[1,2,3,4,5] Hua Jin,[1,2,3,4,5] Chunpan Zhang,[1,2,3,4,5] Mengyi Li,[1,5] Zhongtao Zhang,[1,5] Songlin Wang,[2,6] Dong Zhang,[1,2,3,4,5,6] and Guangyong Sun[1,2,3,4,5,6]

[1]General Surgery Department, Beijing Friendship Hospital, Capital Medical University, Beijing; [2]Immunology Research Center for Oral and Systemic Health, Beijing Friendship Hospital, Capital Medical University, Beijing; [3]Beijing Key Laboratory of Tolerance Induction and Organ Protection in Transplantation, Beijing; [4]Beijing Clinical Research Institute, Beijing; [5]National Clinical Research Center for Digestive Diseases, Beijing; and [6] Beijing Laboratory of Oral Health, Capital Medical University School of Basic Medicine, Beijing, China

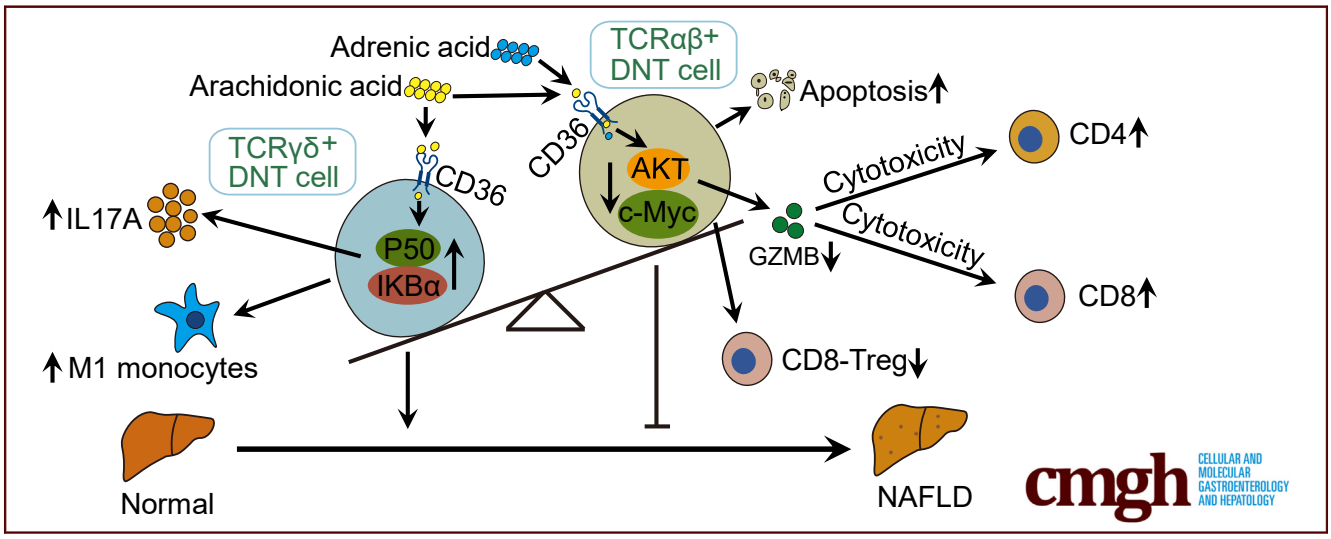

SUMMARY

During NAFLD development, the proportion of TCR$\alpha\beta^+$ DNT cells decreased, whereas TCR$\gamma\delta^+$ DNT cells increased significantly. TCR$\gamma\delta^+$ DNT cells enhance IL17A secretion and aggravate liver inflammation, whereas TCR$\alpha\beta^+$ DNT cells decrease GZMB production and lead to weakened immunoregulation in NAFLD.

BACKGROUND & AIMS: Hepatic inflammation is a hallmark of nonalcoholic fatty liver disease (NAFLD). Double negative T (DNT) cells are a unique subset of T lymphocytes that do not express CD4, CD8, or natural killer cell markers, and studies have suggested that DNT cells play critical and diverse roles in the immune system. However, the role of intrahepatic DNT cells in NAFLD is largely unknown.

METHODS: The proportions and RNA transcription profiling of intrahepatic DNT cells were compared between C57BL/6 mice fed with control diet or methionine-choline–deficient diet for 5 weeks. The functions of DNT cells were tested in vitro and in vivo.

RESULTS: The proportion of intrahepatic DNT cells was significantly increased in mice with diet-induced NAFLD. In NAFLD mice, the proportion of intrahepatic TCR$\gamma\delta^+$ DNT cells was increased along with elevated interleukin (IL) 17A; in contrast, the percentage of TCR$\alpha\beta^+$ DNT cells was decreased, accompanied by reduced granzyme B (GZMB). TCR$\gamma\delta^+$ DNT cell depletion resulted in lowered liver IL17A levels and significantly alleviated NAFLD. Adoptive transfer of intrahepatic TCR$\alpha\beta^+$ DNT cells from control mice increased intrahepatic CD4 and CD8 T cell apoptosis and inhibited NAFLD progression. Furthermore, we revealed that adrenic acid and arachidonic acid, harmful fatty acids that were enriched in the liver of the mice with NAFLD, could induce apoptosis of TCR$\alpha\beta^+$ DNT cells and inhibit their immunosuppressive function and nuclear factor kappa B (NF-κB) or AKT signaling pathway activity. However, arachidonic acid facilitated IL17A secretion by TCR$\gamma\delta^+$ DNT cells, and the NF-κB signaling pathway was involved. Finally, we also confirmed the variation

of intrahepatic TCR$\alpha\beta^+$ DNT cells and TCR$\gamma\delta^+$ DNT cells in humans.

CONCLUSIONS: During NAFLD progression, TCR$\gamma\delta^+$ DNT cells enhance IL17A secretion and aggravate liver inflammation, whereas TCR$\alpha\beta^+$ DNT cells decrease GZMB production and lead to weakened immunoregulatory function. Shifting of balance from TCR$\gamma\delta^+$ DNT cell response to one that favors TCR$\alpha\beta^+$ DNT regulation would be beneficial for the prevention and treatment of NAFLD. *(Cell Mol Gastroenterol Hepatol 2022;13:1805–1827; https://doi.org/10.1016/j.jcmgh.2022.02.019)*

Keywords: NAFLD; TCR$\alpha\beta^+$ DNT Cells; TCR$\gamma\delta^+$ DNT Cells; IL17A; GZMB.

Nonalcoholic fatty liver disease (NAFLD) is one of the most important causes of liver disease worldwide.[1] NAFLD is driven by a combination of genetic and lifestyle factors and involves excessive liver fat accumulation or progression to necroinflammation (nonalcoholic steatohepatitis [NASH]) or fibrosis to cirrhosis and eventually hepatocellular carcinoma.[2] Although a wealth of information on the pathogenesis of NAFLD/NASH is available, no specific treatments have been approved by regulatory agencies.[2,3]

The liver is an important immune organ with many immune cells, and the interaction between innate and adaptive immune cells plays a critical role in the pathogenesis and progression of NAFLD/NASH.[4,5] Double negative T (DNT) cells are a unique subset of T lymphocytes that do not express CD4, CD8, or natural killer cell markers. Although DNT cells account for only a small proportion of total T lymphocytes in the peripheral blood and lymph organs of humans and mice, an increasing number of studies have suggested that this unique T-cell population plays critical and diverse roles in the immune system.[6–8]

Some reports have indicated that DNT cells highly express perforin, granzyme B (GZMB), and Fas ligand and strongly restrain CD4$^+$ and CD8$^+$ T cells,[9–12] as well as B cells,[13,14] dendritic cells,[15] and natural killer cells,[16] thus regulating antigen-specific T-cell responses and various immune responses.[9,17,18] However, several lines of evidence suggest that DNT cells can aggravate the pathogenesis of autoimmune disorders by producing abundant levels of the proinflammatory cytokine interleukin 17 (IL17) in patients with systemic lupus erythematosus and autoimmune disorders such as primary Sjögren's syndrome.[19–21] Overall, current studies strongly support the notion that DNT cells are composed of a rare but heterogeneous T-lymphocyte subset.

We recently demonstrated that the adoptive transfer of ex vivo-generated CD4$^+$ T cell–converted DNT cells ameliorated the development of NASH by inhibiting liver-infiltrating Th17 cells and proinflammatory M1 macrophages.[22] However, the role of intrahepatic natural DNT cells in the development and progression of NAFLD/NASH is still unknown. In this study, we found that DNT cells consist of TCR$\gamma\delta^+$ DNT cells and TCR$\alpha\beta^+$ DNT cells. The balance of TCR$\gamma\delta^+$ and TCR$\alpha\beta^+$ DNT cells plays critical roles in maintaining hepatic immune homeostasis. During NAFLD development, TCR$\gamma\delta^+$ DNT cells enhance IL17A secretion and aggravate liver inflammation, whereas TCR$\alpha\beta^+$ DNT cells decrease GZMB production and lead to weakened immunoregulatory function. Shifting the balance toward hepatic inflammation promotes the progression of NAFLD/NASH.

Results

The Proportion and Number of Hepatic DNT Cells Increased Rapidly in Mice With NAFLD

The percentage of DNT cells in total T cells in the liver was markedly higher than that in the spleen, peripheral blood, axillary lymph nodes (ALNs), draining lymph nodes from the liver (DLNs), mesenteric lymph nodes (MLNs), and inguinal lymph nodes (ILNs), suggesting that DNT cells might exert critical roles in the liver immune system (Figure 1*A*). To study the proportion of DNT cells in NAFLD, we used a mouse model of methionine-choline–deficient (MCD)-induced NAFLD. As shown in Figure 1*B* and *C*, H&E staining and Oil Red O and α-SMA staining displayed more severe inflammation, lipid droplet accumulation, and liver fibrosis in the MCD-fed mice than in the normal control diet (NCD)-fed mice. Serum alanine aminotransferase (ALT) and aspartate aminotransferase (AST) significantly increased in the MCD-fed mice (Figure 1*D*). Interestingly, flow cytometric analysis also showed that the proportion of DNT (CD3$^+$CD4$^-$CD8$^-$NK1.1$^-$) cells in CD3$^+$ T cells and CD45$^+$ cells in the liver increased in the MCD-fed mice compared with the NCD-fed mice (Figure 1*E*). Although the absolute number of intrahepatic DNT cells in the MCD-fed mice was higher than that in the NCD-fed mice (Figure 1*F*), flow cytometry showed that the apoptosis of intrahepatic DNT cells increased significantly in the MCD-fed mice compared with the NCD-fed mice, whereas the intrahepatic DNT cell proliferation in the MCD-fed mice did not change significantly (Figure 1*G*). Moreover, the proportion of DNT cells in CD3$^+$ T cells in the spleen decreased but increased in the blood. The proportions of DNT cells in the ALNs, DLNs, and MLNs in the MCD-fed mice were comparable with those in the NCD-fed mice (Figure 1*H*).

***Authors share co-first authorship.**

Abbreviations used in this paper: **AA, arachidonic acid; ADA, adrenic acid; ALN, axillary lymph node; ALT, alanine aminotransferase; AST, aspartate aminotransferase; CDHFD, choline-deficient, high-fat diet; Cxcl16, CXCR6 ligand 16; CXCR6, chemokine (C-X-C motif) receptor 6; DLN, draining lymph node; DNT, double negative T; FA, fatty acid; GO, Gene Ontology; GSEA, gene set enrichment analysis; GZMB, granzyme B; IHC, immunohistochemistry; IL17A, interleukin 17A; ILN, inguinal lymph node; KEGG, Kyoto Encylopedia of Genes and Genomics; MCD, methionine-choline–deficient; MLN, mesenteric lymph node; NAFLD, nonalcoholic fatty liver disease; NASH, nonalcoholic steatohepatitis; NCD, normal control diet; NF-κB, nuclear factor kappa B; PCR, polymerase chain reaction; PI3K-AKT, phosphatidylinositol 3-kinase- protein kinase B; TFBS, transcription factor binding site.**

Most current article

2352-345X
https://doi.org/10.1016/j.jcmgh.2022.02.019

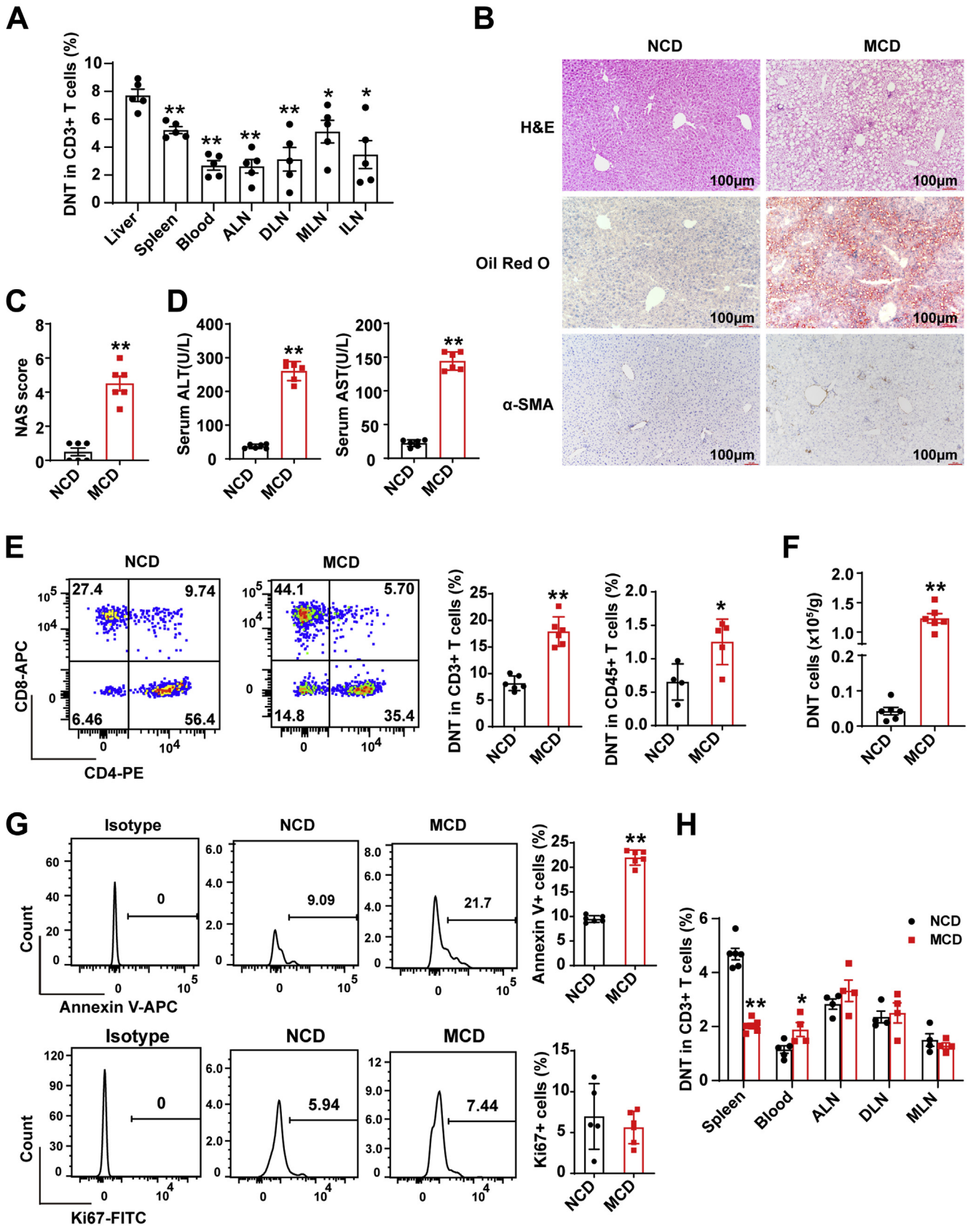
A
DNT in CD3+ T cells (%)
Liver
Spleen
Blood
ALN
DLN
MLN
ILN
B
NCD
MCD
H&E
Oil Red O
α-SMA
100μm
C
NAS score
D
Serum ALT(U/L)
Serum AST(U/L)
E
CD8-APC
CD4-PE
27.4
9.74
6.46
56.4
44.1
5.70
14.8
35.4
DNT in CD3+ T cells (%)
DNT in CD45+ T cells (%)
F
DNT cells (x10⁵/g)
G
Isotype
Count
Annexin V-APC
Annexin V+ cells (%)
Ki67-FITC
Ki67+ cells (%)
H
DNT in CD3+ T cells (%)
Spleen
Blood
ALN
DLN
MLN

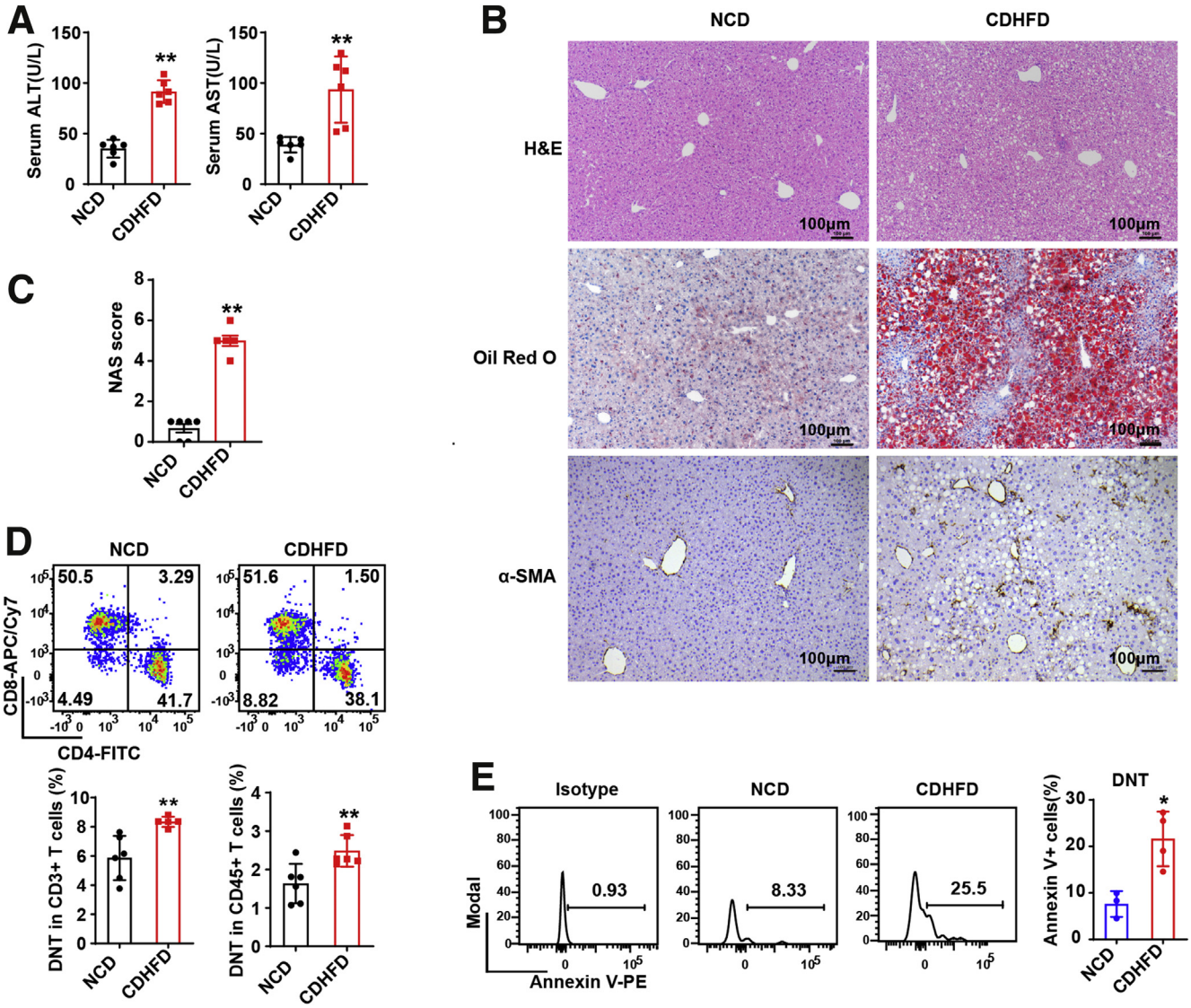

Figure 2. Proportion of DNT cells increased in CDHFD-induced NAFLD. (*A*) Serum ALT and serum AST were measured in NCD- and CDHFD-fed mice. (*B*) Representative H&E staining and Oil Red O and α-SMA staining in livers of NCD- and CDHFD-fed mice. (*C*) NAFLD activity score (NAS) in livers of NCD and CDHFD mice. (*D*) Representative flow cytometry plots and statistical analysis of percentages of intrahepatic DNT cells in $CD3^+$ T cells and $CD45^+$ T cells of NCD- and CDHFD-fed mice. (*E*) Representative flow cytometry plots and statistical analysis of annexin V^+ expression in intrahepatic DNT cells in NCD- and CDHFD-fed mice. n $\geq$ 3 mice/group. Two-sided *P* values <.05 were considered significant. $^{**}P < .01$; $^{*}P < .05$.

We also established NAFLD mouse models with a choline-deficient high-fat diet (CDHFD) for 18 weeks (Figure 2*A*–*C*). The proportions of intrahepatic DNT cells in $CD3^+$ T cells and $CD45^+$ cells were also increased in the CDHFD-fed mice, and annexin V analysis showed significantly increased apoptosis of DNT cells in the CDHFD-fed mice (Figure 2*D* and *E*). These observations indicated that the proportions, numbers, and apoptosis rate of intrahepatic DNT cells increased markedly in NAFLD.

Figure 1. (***See previous page***). **Proportion of DNT cells increased in MCD-induced NAFLD for 5 weeks.** (*A*) Percentages of DNT cells in $CD3^+$ T cells among the liver, spleen, blood, ALNs, DLNs, MLNs, and ILNs from normal mice. (*B*) Representative H&E staining and Oil Red O and α-SMA staining in livers of NCD- and MCD-fed mice. (*C*) NAFLD activity score (NAS) in livers of NCD and MCD mice. (*D*) Serum ALT and serum AST were measured in NCD- and MCD-fed mice. (*E*) Representative flow cytometry plots and statistical analysis of percentages of intrahepatic DNT cells in $CD3^+$ T cells and $CD45^+$ T cells of NCD- and MCD-fed mice. (*F*) Numbers of intrahepatic DNT cells in NCD- and MCD-fed mice. (*G*) Representative flow cytometry plots and statistical analysis of annexin V^+ and $Ki67^+$ expression in intrahepatic DNT cells in NCD- and MCD-fed mice. (*H*) Percentages of DNT cells in $CD3^+$ T cells among the spleen, blood, ALNs, DLNs, and MLNs of NCD- and MCD-fed mice. n $\geq$ 4 mice/group. Two-sided *P* values <.05 were considered significant. $^{**}P < .01$; $^{*}P < .05$.

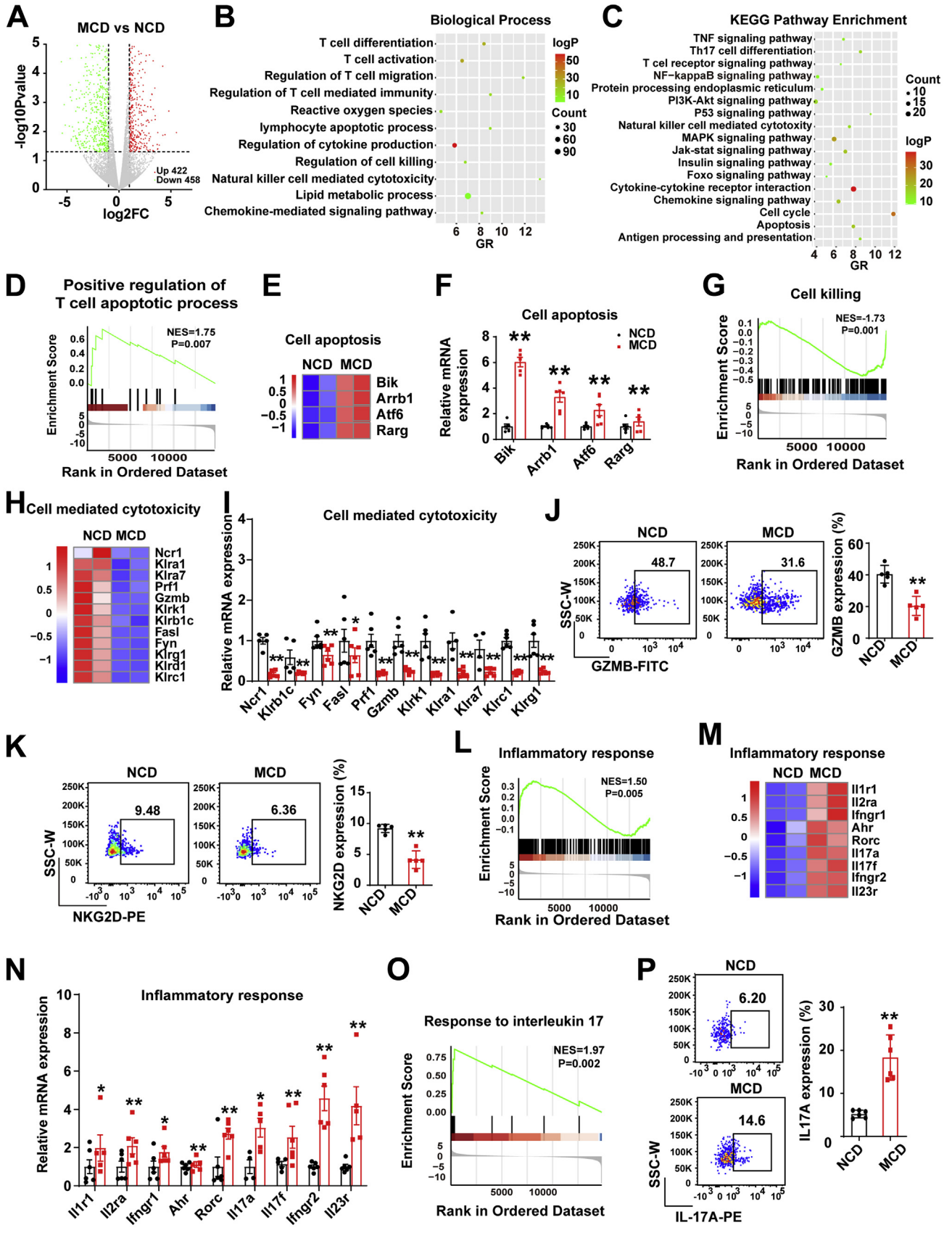
A
MCD vs NCD
-log10Pvalue
log2FC
Up 422
Down 458
B
Biological Process
T cell differentiation
T cell activation
Regulation of T cell migration
Regulation of T cell mediated immunity
Reactive oxygen species
lymphocyte apoptotic process
Regulation of cytokine production
Regulation of cell killing
Natural killer cell mediated cytotoxicity
Lipid metabolic process
Chemokine-mediated signaling pathway
logP
Count
GR
C
KEGG Pathway Enrichment
TNF signaling pathway
Th17 cell differentiation
T cel receptor signaling pathway
NF−kappaB signaling pathway
Protein processing endoplasmic reticulum
PI3K-Akt signaling pathway
P53 signaling pathway
Natural killer cell mediated cytotoxity
MAPK signaling pathway
Jak-stat signaling pathway
Insulin signaling pathway
Foxo signaling pathway
Cytokine-cytokine receptor interaction
Chemokine signaling pathway
Cell cycle
Apoptosis
Antigen processing and presentation
Count
logP
GR
D
Positive regulation of T cell apoptotic process
NES=1.75
P=0.007
Enrichment Score
Rank in Ordered Dataset
E
Cell apoptosis
NCD MCD
Bik
Arrb1
Atf6
Rarg
F
Cell apoptosis
Relative mRNA expression
NCD
MCD
Bik
Arrb1
Atf6
Rarg
G
Cell killing
NES=-1.73
P=0.001
Enrichment Score
Rank in Ordered Dataset
H
Cell mediated cytotoxicity
NCD MCD
Ncr1
Klra1
Klra7
Prf1
Gzmb
Klrk1
Klrb1c
Fasl
Fyn
Klrg1
Klrd1
Klrc1
I
Cell mediated cytotoxicity
Relative mRNA expression
Ncr1
Klrb1c
Fyn
Fasl
Prf1
Gzmb
Klrk1
Klra1
Klra7
Klrc1
Klrg1
J
NCD
MCD
48.7
31.6
SSC-W
GZMB-FITC
GZMB expression (%)
NCD
MCD
K
NCD
MCD
9.48
6.36
SSC-W
NKG2D-PE
NKG2D expression (%)
NCD
MCD
L
Inflammatory response
NES=1.50
P=0.005
Enrichment Score
Rank in Ordered Dataset
M
Inflammatory response
NCD MCD
Il1r1
Il2ra
Ifngr1
Ahr
Rorc
Il17a
Il17f
Ifngr2
Il23r
N
Inflammatory response
Relative mRNA expression
Il1r1
Il2ra
Ifngr1
Ahr
Rorc
Il17a
Il17f
Ifngr2
Il23r
O
Response to interleukin 17
NES=1.97
P=0.002
Enrichment Score
Rank in Ordered Dataset
P
NCD
MCD
6.20
14.6
SSC-W
IL-17A-PE
IL17A expression (%)
NCD
MCD

Transcriptome Sequencing Analysis of Intrahepatic DNT Cells in the NCD- and MCD-Fed Mice

To further elucidate the function of intrahepatic DNT cells in NAFLD, we compared DNT cells from the livers of the MCD- and NCD-fed mice in a transcriptome sequencing study. The volcano study showed that DNT cells in the MCD-fed mice had 880 differentially expressed genes (P value $<.05$ and fold change ≤ 0.5 or fold change ≥ 1.5) compared with the NCD-fed mice (Figure 3*A*). Gene Ontology (GO) and Kyoto Encyclopedia of Genes and Genomics (KEGG) pathway analyses revealed that the differentially expressed genes were involved in T-cell activation, regulation of lymphocyte apoptotic process, cytokine production, cell killing, positive regulation of natural killer cell–mediated cytotoxicity, lipid metabolic process, and apoptosis among others. In addition, various signaling pathways, such as the phosphatidylinositol 3-kinase (PI3K)-protein kinase B (AKT) and nuclear factor kappa B (NF-κB) signaling pathways, were involved (Figure 3*B* and *C*). Analysis of all genes in DNT cells and gene set enrichment analysis (GSEA) of DNT cells showed that positive regulation of the T-cell apoptotic process was increased (NES = 1.75, $P = .007$) (Figure 3*D*). Moreover, compared with that in the NCD-fed mice, the expression of apoptosis-related genes (*Bik*, *Arrb1*, *Atf6,* and *Rarg*) in DNT cells was increased, and the changes in these genes were validated through real-time polymerase chain reaction (PCR) (Figure 3*E* and *F*). Together, these data indicated that the apoptosis of intrahepatic DNT cells increased in NAFLD and that the AKT and NF-κB signaling pathways may be involved.

Compared With the NCD-Fed Mice, the MCD-Fed Mice Exhibited Decreased Immunosuppressive Functions of Intrahepatic DNT Cells and Enhanced Proinflammatory Response

To explore the function of intrahepatic DNT cells during NAFLD development, we analyzed the cytotoxicity and inflammatory response of DNT cells. GSEA showed that the cell killing of DNT cells in the MCD-fed mice declined significantly compared with that in the NCD-fed mice (Figure 3*G*). The levels of cell-mediated cytotoxicity genes, such as *Ncr1, Klrb1c, Fyn, Fasl, Klrc2, Klra3, Klra9, Prf1, Gzmb, Klrk1, Klra1, Klra7, Klrd1,* and *Klrc1,* in DNT cells of the MCD-fed mice were down-regulated sharply (Figure 3*H* and *I*). As expected, flow cytometry also showed that GZMB expression decreased in DNT cells of the MCD-fed mice compared with the NCD-fed mice (Figure 3*J*), which indicated that the suppressive function of DNT cells decreased. We also observed that the expression of NKG2D (encoded by *Klrk1*) decreased significantly, which indicated that DNT cells may be involved in inhibitory conditions during NAFLD development (Figure 3*K*).

GSEA also showed that the inflammatory response of intrahepatic DNT cells was markedly enhanced in the MCD-fed mice compared with NCD-fed mice (NES = 1.50, $P = .005$) (Figure 3*L*). Some inflammatory response genes, such as *Il1r1, Il2ra, Ifngr1, Ahr, Rorc, Il17a, Il17f, Ifngr2,* and *Il23r,* showed increased expression (Figure 3*M* and *N*). Interestingly, GSEA of intrahepatic DNT cells showed that the IL17 pathway was increased (Figure 3*O*). Flow cytometry also showed that IL17A secretion in intrahepatic DNT cells from the MCD-fed mice was increased dramatically compared with that in the NCD-fed mice (Figure 3*P*).

TCR$\alpha\beta^+$ DNT Cells Mainly Decreased GZMB Production, Whereas TCR$\gamma\delta^+$ DNT Cells Mainly Enhanced IL17A Secretion During NAFLD Development

To further determine the function of different DNT cell subsets in NAFLD, we assessed DNT cells with TCRβ chains and TCR$\gamma\delta$ chains (Figure 4*A*). As shown in Figure 4*B*, the DNT cells included CD4 and CD8 double negative TCR$\alpha\beta^+$ and TCR$\gamma\delta^+$ cells. The proportion of TCR$\alpha\beta^+$ DNT cells decreased significantly, whereas TCR$\gamma\delta^+$ DNT cells increased obviously during NAFLD development. Annexin V staining showed that the apoptosis of TCR$\alpha\beta^+$ DNT cells was heavily increased

Figure 3. (***See previous page***). **RNA-sequencing showed the differentially expressed genes and biological function of DNT cells from livers of MCD-fed mice compared with NCD-fed mice.** (*A*) Differences of genes with up-regulated (422) and down-regulated (458) expression in intrahepatic DNT cells from MCD-fed mice compared with NCD-fed mice; fold change ≤ 0.5 or fold change ≥ 1.5; $P < .05$. (*B* and *C*) Biological Process and KEGG pathway analyses were performed on the basis of the genes with significantly up-regulated and down-regulated expression in intrahepatic DNT cells from MCD-fed mice compared with NCD-fed mice. (*D*) GSEA of positive regulation of the T-cell apoptotic process in intrahepatic DNT cells from MCD-fed mice compared with NCD-fed mice. (*E* and *F*) Heatmap showing up-regulated and down-regulated genes related to cell apoptosis in intrahepatic DNT cells from MCD-fed mice compared with NCD-fed mice. The significantly changed genes related to cell apoptosis were confirmed via real-time PCR. (*G*) GSEA of cell killing in intrahepatic DNT cells of MCD-fed mice. (*H*) Heatmap showing the genes with down-regulated expression related to cell-mediated cytotoxicity in intrahepatic DNT cells from MCD-fed mice compared with NCD-fed mice. (*I*) The significantly changed genes related to cell-mediated cytotoxicity were confirmed via real-time PCR. (*J* and *K*) Representative flow cytometry plots and statistical analysis of GZMB and NKG2D expression in intrahepatic DNT cells from NCD- and MCD-fed mice. (*L*) GSEA of the inflammatory response in intrahepatic DNT cells from NCD- and MCD-fed mice. (*M*) Heatmap showing genes with up-regulated and down-regulated expression related to the inflammatory response in intrahepatic DNT cells from livers of MCD-fed mice compared with NCD-fed mice. (*N*) The significantly changed genes related to the inflammatory response were confirmed via real-time PCR. (*O*) GSEA of the response to IL17 in intrahepatic DNT cells from NCD- and MCD-fed mice. (*P*) Representative flow cytometry plots and statistical analysis of IL17A expression in intrahepatic DNT cells from NCD- and MCD-fed mice. n $\geq$ 5 mice/group. Two-sided P values $<.05$ were considered significant. $^{**}P < .01$; $^{*}P < .05$.

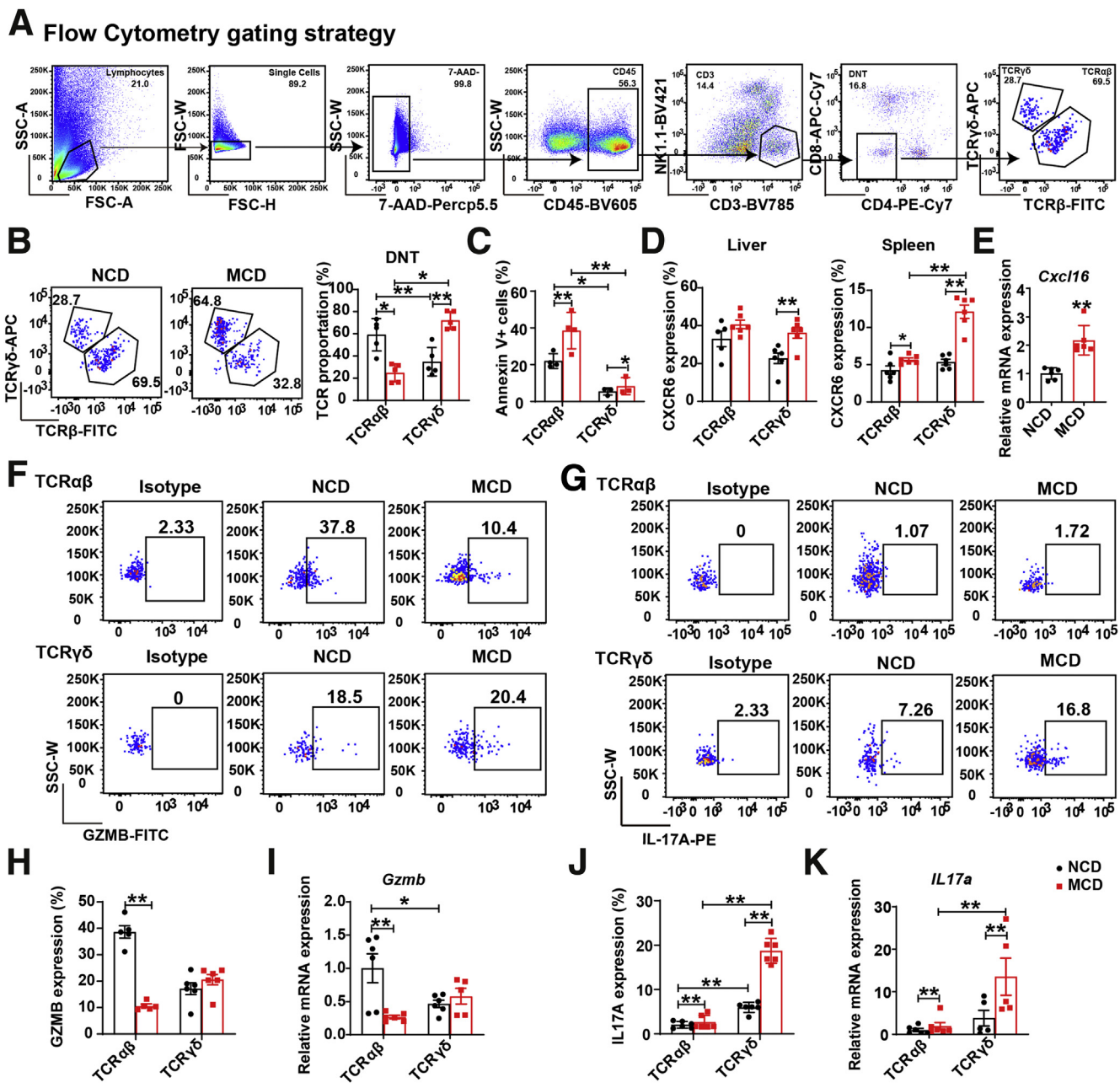

Figure 4. Immunosuppressive function of DNT cells was controlled by TCR$\alpha\beta+$ DNT cells, and secretion of inflammatory factors was controlled by TCR$\gamma\delta^+$ DNT cells. (*A*) Representative flow cytometry gating strategy of TCR proportions in intrahepatic DNT cells. (*B*) Representative flow cytometry plots of TCR proportions in intrahepatic DNT cells from MCD- and NCD-fed mice. (*C*) Statistical analysis in apoptosis of TCR subtypes in intrahepatic DNT cells from MCD- compared with NCD-fed mice by flow cytometry. n = 3 mice/group. (*D*) Statistical analysis by flow cytometry of CXCR6 expression in liver and spleen TCR$\gamma\delta^+$ DNT cells and TCR$\alpha\beta^+$ DNT cells among NCD- and MCD-fed mice. (*E*) The mRNA expression of Cxcl16 in liver among NCD- and MCD-fed mice. (*F*, *H*, and *I*) Representative flow cytometry plots and mRNA of GZMB expression in intrahepatic TCR$\gamma\delta^+$ DNT cells and TCR$\alpha\beta^+$ DNT cells among NCD- and MCD-fed mice. (*G*, *J*, and *K*) Representative flow cytometry plots and mRNA of IL17A expression in intrahepatic TCR$\gamma\delta^+$ DNT cells and TCR$\alpha\beta^+$ DNT cells from NCD- and MCD-fed mice. n $\geq$ 5 mice/group. Two-sided P values $<$.05 were considered significant. $^{**}P < .01$; $^{*}P < .05$.

compared with that of TCR$\gamma\delta^+$ cells in the MCD-fed mice (Figure 4*C*). Although chemokine (C-X-C motif) receptor 6 (CXCR6) expression increased in TCR$\gamma\delta^+$ DNT cells from the spleen and the liver in MCD-fed mice, we also confirmed that the corresponding chemokine C-X-C motif chemokine ligand 16 (Cxcl16) increased markedly in the liver at the mRNA level (Figure 4*D* and *E*), so we believe the elevation of TCR$\gamma\delta^+$ DNT cells in MCD-fed liver is due to the migration of these cells from the spleen. These differences in TCR$\alpha\beta^+$ and TCR$\gamma\delta^+$ DNT cell survival and CXCR6 expression may induce changes in the proportions of DNT subsets during NAFLD development.

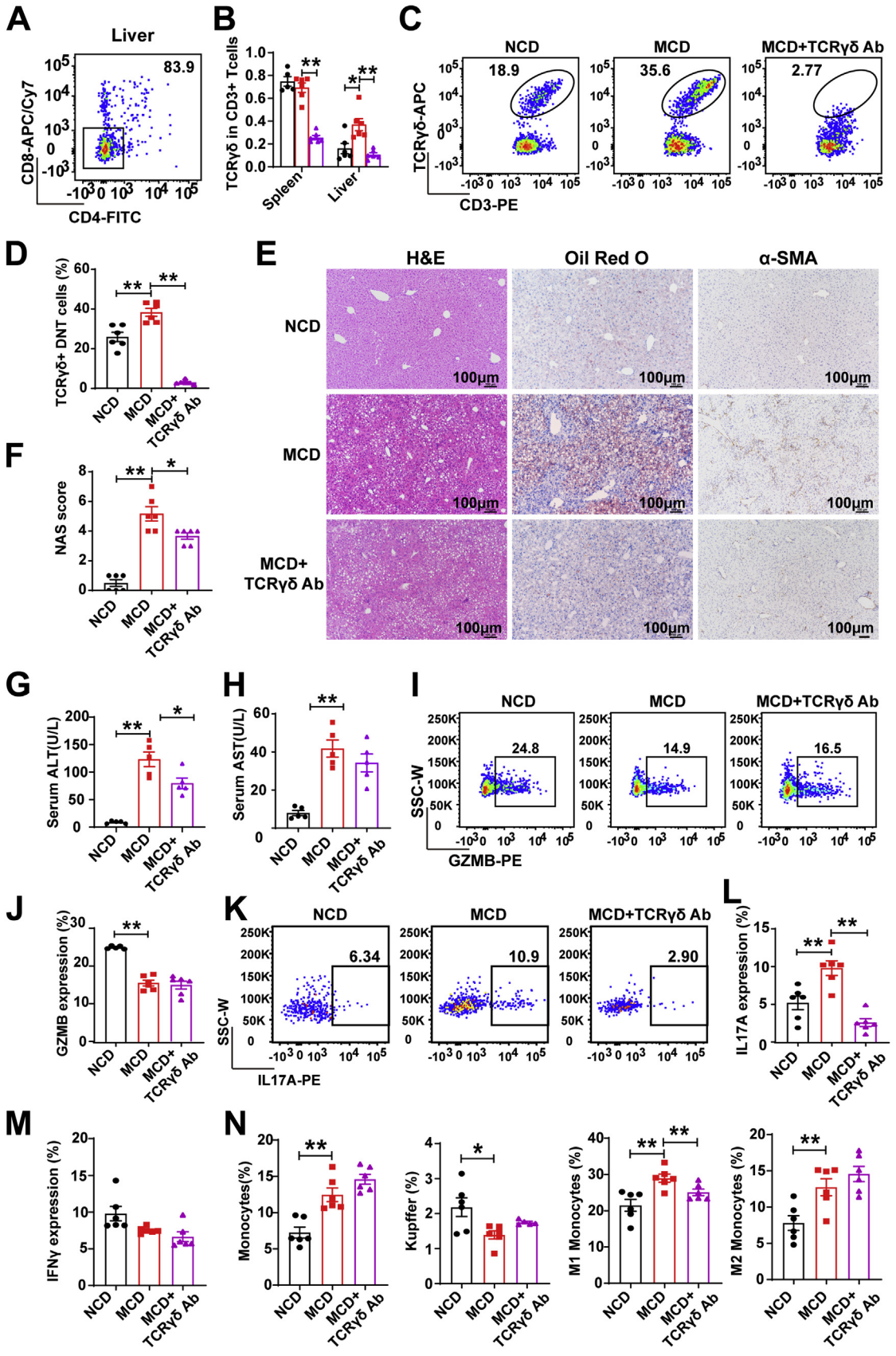
A
Liver
83.9
CD8-APC/Cy7
CD4-FITC
B
TCRγδ in CD3+ Tcells
Spleen
Liver
C
NCD
MCD
MCD+TCRγδ Ab
18.9
35.6
2.77
TCRγδ-APC
CD3-PE
D
TCRγδ+ DNT cells (%)
NCD
MCD
MCD+ TCRγδ Ab
E
H&E
Oil Red O
α-SMA
NCD
MCD
MCD+ TCRγδ Ab
100μm
F
NAS score
G
Serum ALT(U/L)
H
Serum AST(U/L)
I
24.8
14.9
16.5
SSC-W
GZMB-PE
J
GZMB expression (%)
K
6.34
10.9
2.90
IL17A-PE
L
IL17A expression (%)
M
IFNγ expression (%)
N
Monocytes(%)
Kupffer (%)
M1 Monocytes (%)
M2 Monocytes (%)

Flow cytometry also showed that GZMB expression in TCR$\alpha\beta^+$ DNT cells was higher than that in TCR$\gamma\delta^+$ DNT cells of the NCD-fed mice. During NAFLD development, GZMB expression in TCR$\alpha\beta^+$ DNT cells decreased significantly but did not change in TCR$\gamma\delta^+$ DNT cells (Figure 4*F*, *H*, and *I*). These results suggested that the decreased DNT cell suppressive function during NAFLD development was mainly caused by TCR$\alpha\beta^+$ DNT cells.

We also found a markedly elevated expression of IL17A produced in TCR$\gamma\delta^+$ DNT cells but not in TCR$\alpha\beta^+$ DNT cells, which indicated that the increased IL17A secretion from intrahepatic DNT cells in the MCD-fed mice was mainly from TCR$\gamma\delta^+$ DNT cells (Figure 4*G*, *J*, and *K*). Taken together, these observations suggest that TCR$\alpha\beta^+$ DNT cells decrease GZMB production, commonly leading to weakened immunoregulatory function during NAFLD progression, whereas TCR$\gamma\delta^+$ DNTs enhance IL17A secretion and aggravate liver inflammation.

TCR$\gamma\delta^+$ DNT Depletion Resulted in Lowered Liver IL17A Levels and Significantly Alleviated NAFLD

CD4$^-$CD8$^-$ cells accounted for 83.9% of hepatic TCR$\gamma\delta^+$ T cells (Figure 5*A*). To further confirm the roles of TCR$\gamma\delta^+$ DNT cells during NAFLD development, we used a depletion antibody against TCR$\gamma\delta$ to eliminate TCR$\gamma\delta^+$ DNT cells in the MCD-fed mice. As shown in Figure 5*B*, TCR$\gamma\delta$ T cells in CD3$^+$ T cells were reduced as expected in the spleen and liver in the MCD-fed mice. TCR$\gamma\delta^+$ DNT cells were also significantly decreased in the MCD-fed mice after TCR$\gamma\delta$ depletion (Figure 5*C* and *D*). To further verify the effects of TCR$\gamma\delta$ T-cell depletion in the MCD-fed mice, we examined the liver pathology. As shown in Figure 5*E* and *F*, TCR$\gamma\delta$ depletion decreased liver fat accumulation and lobular inflammation but not α-SMA levels in the MCD-fed mice. We also found that TCR$\gamma\delta$ T-cell elimination lowered serum ALT and AST levels in the mice with NAFLD (Figure 5*G* and *H*).

TCR$\gamma\delta^+$ DNT cell clearance had no effects on GZMB expression in all DNT cells (Figure 5*I* and *J*) but significantly decreased DNT cell IL17A secretion in the MCD-fed mice (Figure 5*K* and *L*). TCR$\gamma\delta^+$ DNT cell clearance had no effects on interferon γ expression in all DNT cells (Figure 5*M*). In addition, we investigated whether TCR$\gamma\delta^+$ DNT cell clearance had any effect on the progression of inflammation. As shown in Figure 5*N*, flow cytometry showed that depleting TCR$\gamma\delta^+$ DNT cells reduced M1 monocyte proportions but not total monocytes, Kupffer cells, or M2 monocytes in the MCD-fed mice. These observations indicated that the clearance of TCR$\gamma\delta^+$ DNT cells decreased IL17A expression but not GZMB expression, ultimately inhibiting hepatic inflammation and NAFLD development.

Adoptive Transfer of TCR$\alpha\beta^+$ DNT Cells Could Regulate the Intrahepatic Immunologic Environment and Prevent NAFLD Development

To further confirm the roles of TCR$\alpha\beta^+$ DNT cells during NAFLD development, we isolated TCR$\alpha\beta^+$ DNT cells from normal mouse liver and then adoptively transferred them into recipient mice. After 5 weeks of MCD feeding, as shown in Figure 6*A*, adoptive transfer of TCR$\alpha\beta^+$ DNT cells significantly reduced serum ALT and AST levels in the MCD-fed mice. H&E, Oil Red O, and α-SMA staining also demonstrated that TCR$\alpha\beta^+$ DNT cell transfer significantly decreased liver fat accumulation, lobular inflammation, and liver fibrosis (Figure 6*B* and *C*). In addition, we found that intrahepatic PD-1$^+$CD122$^+$CD8$^+$ Treg cells but not FoxP3$^+$CD4$^+$ Treg cells increased after administration of TCR$\alpha\beta^+$ DNT cells (Figure 6*D*–*F*). TCR$\alpha\beta^+$ DNT cells induced intrahepatic T-cell apoptosis, especially CD8$^+$ T cells, in the MCD-fed mice (Figure 6*G*). These observations indicated that TCR$\alpha\beta^+$ DNT cells could regulate the liver immunologic environment and inhibit NAFLD development.

Harmful Fatty Acids Inhibited the TCR$\alpha\beta^+$ DNT Cell Immunosuppressive Functions but Facilitated TCR$\gamma\delta^+$ DNT Cell IL17A Secretion

GSEA showed that fatty acid (FA) metabolism was increased in intrahepatic DNT cells of the MCD-fed mice (NES = 1.36, $P = .007$; Figure 7*A*). Bodipy staining (Thermo Fisher, Waltham, MA) also showed FA accumulation in DNT cells of the MCD-fed mice (Figure 7*B*). CD36, a molecule mediating lipid uptake, was markedly increased in intrahepatic DNT cells in the MCD-fed mice compared with the NCD-fed mice, especially in TCR$\gamma\delta^+$ DNT cells, which was

Figure 5. (***See previous page***). **TCR$\gamma\delta^+$ DNT depletion resulted in lowered liver IL17A levels and significantly alleviated diet-induced NAFLD.** (*A*) Representative flow cytometry plots of DNT proportions in TCR$\gamma\delta^+$ T cells. (*B*) Statistical analysis of TCR$\gamma\delta^+$ T cells in CD3$^+$ T cells from the spleen and liver of NCD- and MCD-fed mice and TCR$\gamma\delta^+$ DNT-depleted mice. (*C* and *D*) Representative flow cytometry plots and statistical analysis of TCR$\gamma\delta^+$ T cells in intrahepatic DNT cells of NCD- and MCD-fed mice and TCR$\gamma\delta^+$ DNT-depleted mice. (*E*) Representative H&E staining and Oil Red O and α-SMA staining in livers of NCD- and MCD-fed mice and TCR$\gamma\delta^+$ DNT-depleted mice. (*F*) NAFLD activity score (NAS) in livers of NCD- and MCD-fed mice and TCR$\gamma\delta^+$ DNT-depleted mice. (*G* and *H*) Serum ALT and serum AST were measured in livers from NCD- and MCD-fed mice and TCR$\gamma\delta^+$ DNT-depleted mice. (*I*–*L*) Representative flow cytometry plots and statistical analysis of GZMB and IL17A expression in intrahepatic DNT cells from NCD- and MCD-fed mice and TCR$\gamma\delta$+ DNT-depleted mice. (*M*) Statistical analysis of interferon γ expression in intrahepatic DNT cells from NCD- and MCD-fed mice and TCR$\gamma\delta^+$ DNT-depleted mice by flow cytometry. (*N*) Proportions of monocytes (CD45$^+$Ly6G$^-$F4/80^{int}CD11b^{hi}), Kupffer cells (CD45$^+$Ly6G$^-$F4/80^{hi}CD11b^{int}), M1 monocytes (CD45$^+$Ly6G$^-$F4/80^{int}CD11b^{hi}CD11c$^+$CD206$^-$), and M2 monocytes (CD45$^+$Ly6G$^-$F4/80^{int}CD11b^{hi}CD11c$^-$CD206$^+$) among intrahepatic DNT cells from NCD- and MCD-fed mice and TCR$\gamma\delta^+$ DNT-depleted mice. n $\geq$ 5 mice/group. Two-sided *P* values $<$.05 were considered significant. $^{**}P < .01$; $^{*}P < .05$.

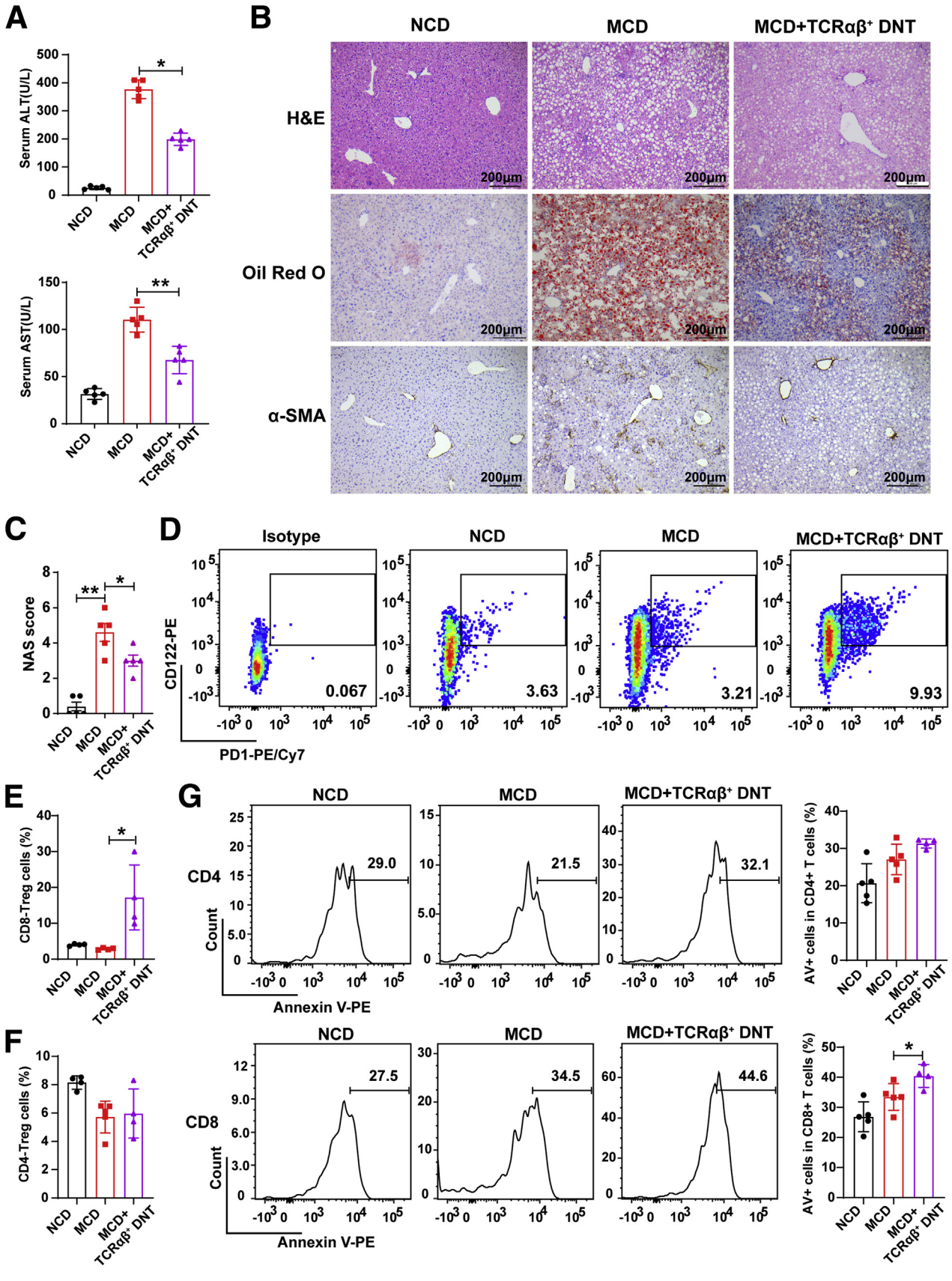
A
Serum ALT(U/L)
Serum AST(U/L)
NCD
MCD
MCD+ TCRαβ+ DNT
B
NCD
MCD
MCD+TCRαβ+ DNT
H&E
Oil Red O
α-SMA
200μm
C
NAS score
D
Isotype
NCD
MCD
MCD+TCRαβ+ DNT
CD122-PE
PD1-PE/Cy7
0.067
3.63
3.21
9.93
E
CD8-Treg cells (%)
F
CD4-Treg cells (%)
G
CD4
CD8
Count
Annexin V-PE
29.0
21.5
32.1
27.5
34.5
44.6
AV+ cells in CD4+ T cells (%)
AV+ cells in CD8+ T cells (%)

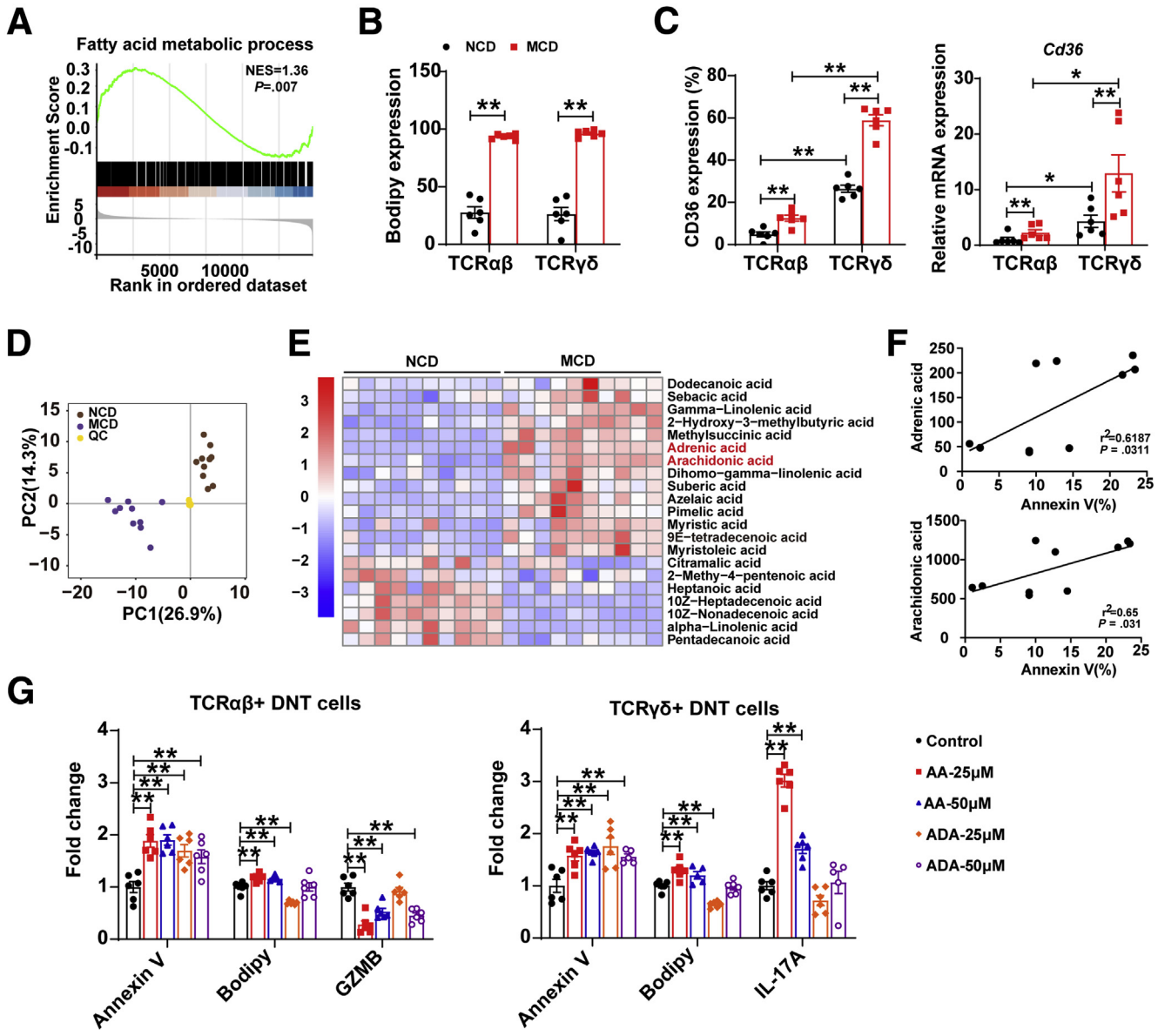

Figure 7. FAs are involved in regulating apoptosis and the function of TCR subtypes of DNT cells. (*A*) GSEA of the response to FA metabolism. (*B*) The level of Bodipy in intrahepatic TCR$\alpha\beta^+$ DNT cells and TCR$\gamma\delta^+$ DNT cells in NCD- and MCD-fed mice. n = 6 mice/group. (*C*) CD36 expression in intrahepatic DNT cells of NCD- and MCD-fed mice by flow cytometry and real-time PCR. n = 6 mice/group. (*D*) Principal component analysis of metabonomics in livers of NCD- and MCD-fed mice. (*E*) FA content in livers of NCD- and MCD-fed mice. n = 6 mice/group. (*F*) Correlation between the harmful FAs ADA, AA levels, and DNT cell apoptosis. n = 9 mice/group. (*G*) Apoptosis, Bodipy, GZMB, IL17A expression in TCR$\gamma\delta^+$ and TCR$\alpha\beta^+$ DNT cells after ADA and AA stimulation. n = 6 biologically independent samples per group. Two-sided *P* values <.05 were considered significant. $^{**}P < .01$; $^{*}P < .05$.

consistent with the real-time PCR results (Figure 7*C*). These observations indicated that the FA metabolic process may play important roles in DNT cells during NAFLD development.

To further explore which FAs affect DNT cell survival and function, we assessed liver samples from the NCD- and MCD-fed mice by metabonomics. Principal component analysis of metabonomics showed that the different

Figure 6. (***See previous page***). **Adoptive transfer of TCR$\alpha\beta^+$ DNT cells prevented the development and progression of NAFLD.** (*A*) Serum ALT and serum AST levels were measured in NCD- and MCD-fed mice and TCR$\alpha\beta^+$ DNT cell-transferred mice. (*B*) Representative H&E staining and Oil Red O and α-SMA staining in livers from NCD- and MCD-fed mice and TCR$\alpha\beta^+$ DNT-transferred mice. (*C*) NAFLD activity score (NAS) in livers of NCD- and MCD-fed mice and TCR$\alpha\beta^+$ DNT-transferred mice. (*D–F*) Representative flow cytometry plots and statistical analysis of proportion of $CD4^+$ and $CD8^+$ Treg cells among livers of NCD- and MCD-fed mice and TCR$\alpha\beta^+$DNT cell-transferred mice. (*G*) Representative flow cytometry plots and statistical analysis of apoptosis of intrahepatic $CD4^+$ and $CD8^+$ cells of NCD- and MCD-fed mice and TCR$\alpha\beta^+$DNT cell-transferred mice. n ≥ 4 mice/group. Two-sided *P* values <.05 were considered significant. $^{**}P < .01$; $^{*}P < .05$.

components were distinct from each other (Figure 7*D*). FA metabonomics analysis showed many FAs changed during NAFLD development, especially the harmful FAs; increased adrenic acid (ADA) and arachidonic acid (AA) (Figure 7*E*) were correlated with DNT cell apoptosis (Figure 7*F*), which indicated these FAs might affect DNT cell survival.

To further reveal the potential mechanism of ADA acid and AA in DNT cell survival and function, we stimulated TCR$\alpha\beta^+$ and TCR$\gamma\delta^+$ DNT cells in vitro (Figure 7*G*). Compared with the control, treatment with AA induced DNT cell apoptosis and increased Bodipy content in TCR$\alpha\beta^+$ DNT cells. GZMB expression was markedly down-regulated after

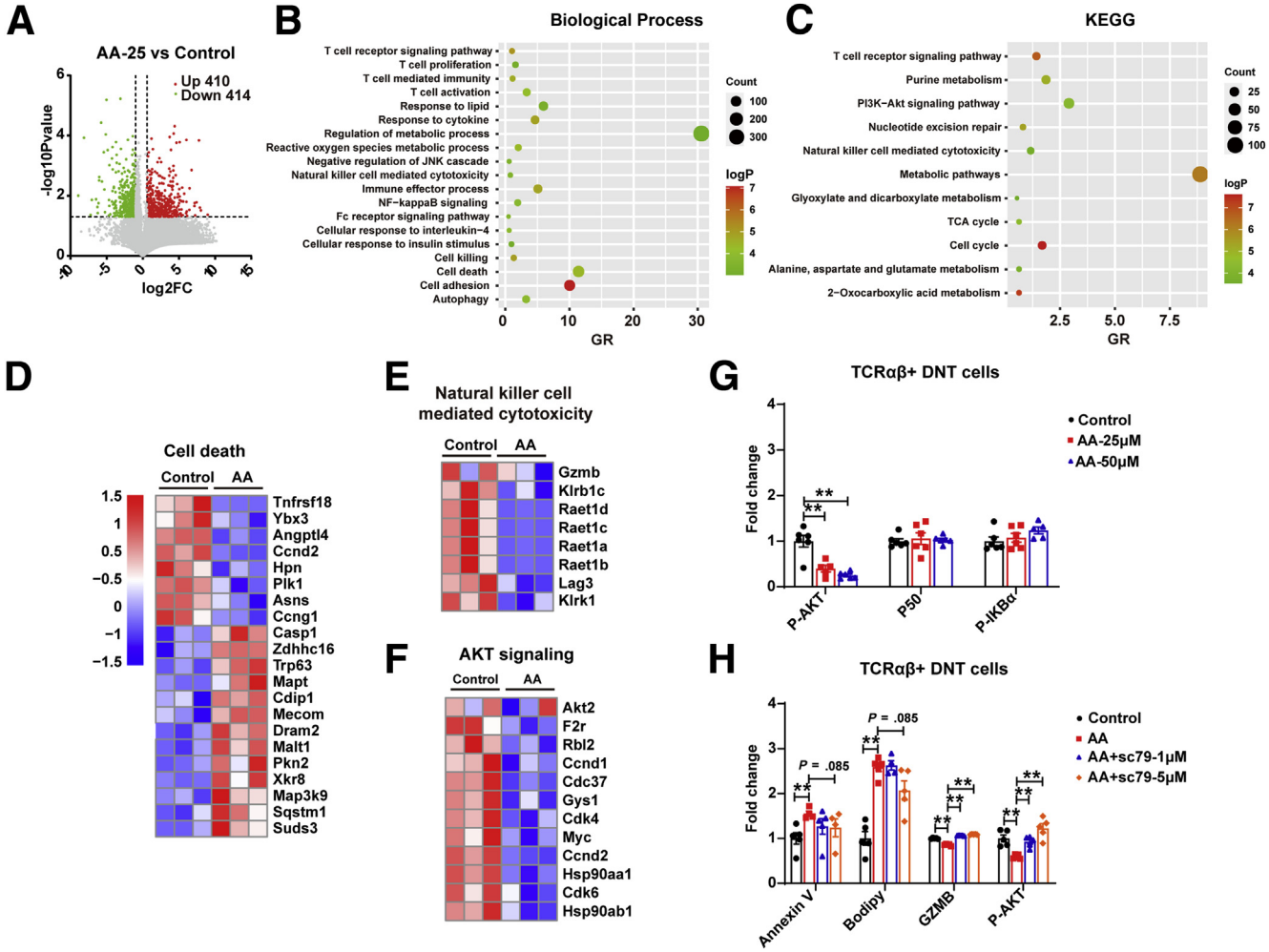

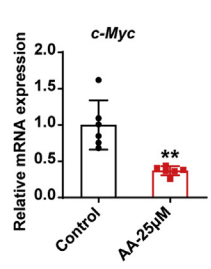

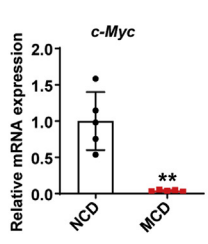

AA stimulation in TCR$\alpha\beta^+$ DNT cells. In addition, treatment with AA enhanced DNT cell apoptosis and increased Bodipy content, IL17A expression in TCR$\gamma\delta^+$ DNT cells. ADA could also induce cell apoptosis and down-regulate GZMB expression in TCR$\alpha\beta^+$ DNT cells but had fewer effects on TCR$\gamma\delta^+$ DNT cells. These data revealed that ADA and AA, harmful FAs that were enriched in the liver of the mice with NAFLD, could induce apoptosis and decrease the immunosuppressive function of TCR$\alpha\beta^+$ DNT cells. However, AA facilitated IL17A secretion by TCR$\gamma\delta^+$ DNT cells.

AA Modulates TCR$\alpha\beta^+$ and TCR$\gamma\delta^+$ DNT Cell Survival and Functions via Different Regulatory Pathways

AA affected GZMB and IL17A secretion by TCR$\alpha\beta^+$ and TCR$\gamma\delta^+$ DNT cells, respectively, and we further focus on the underlying mechanisms. First, transcriptome sequencing was conducted in TCR$\alpha\beta^+$ and TCR$\gamma\delta^+$ DNT cells after stimulating with or without AA for 48 hours. The volcano plot showed TCR$\alpha\beta^+$ DNT cells after AA treatment had 824 differentially expressed genes (P value $<.05$ and fold change ≤ 0.5 or fold change ≥ 1.5) (Figure 8*A*). GO and KEGG pathway enrichment analysis revealed that the significant differentially expressed genes were involved in T-cell activation, regulation of metabolic process, natural killer cell–mediated cytotoxicity, cell death, and PI3K-Akt signaling pathway, among others (Figure 8*B* and *C*). Moreover, compared with control group, the expression of pro-apoptosis genes in TCR$\alpha\beta^+$ DNT cells was up-regulated, whereas the expression of anti-apoptosis genes in TCR$\alpha\beta^+$ DNT cells was down-regulated (Figure 8*D*). In addition, the genes related to natural killer cell–mediated cytotoxicity were decreased, such as *GzmB*, lymphocyte activation gene 3, and others, consistent with those observed in mice (Figure 8*E*). Further investigation demonstrated that PI3K-AKT signaling pathway was enriched, and related genes were down-regulated (Figure 8*F*). In vitro stimulation confirmed that AA can down-regulate P-AKT signaling pathway in a dose-dependent manner (Figure 8*G*). When AKT agonist SC-79 was added, it could partly reverse the effects of AA stimulation, which confirmed the role of AKT signaling pathway in AA regulating TCR$\alpha\beta^+$ DNT cells (Figure 8*H*). To further probe the modulation mechanism of FA AA on GZMB expression in TCR$\alpha\beta^+$ DNT cells, transcription factor binding sites (TFBSs) in the *GzmB* promoter region were also predicted and confirmed by transcription sequencing; the promoter region of *GzmB* includes some TFBSs, such as retinoid X receptor alpha (*Rxra*), signal transducer and activator of transcription 4 (*Stat4*), *Myc*, *Nfkb2*, *Trp53* (Figure 8*I*). We further verified that *c-Myc* was down-regulated after AA treatment and was down-regulated in TCR$\alpha\beta^+$ DNT cells of NAFLD mice liver simultaneously by real-time PCR (Figure 8*J* and *K*). It is well-known that c-Myc was the downstream of PI3K-AKT signaling pathway,[23,24] suggesting that c-Myc may play a critical role in AA regulating GZMB expression.

The volcano plot displayed that TCR$\gamma\delta^+$ DNT cells after treating with AA had 1345 differentially expressed genes (P value $<.05$ and fold change ≤ 0.5 or fold change ≥ 1.5) compared with control (Figure 9*A*). GO analysis revealed that the significant differentially expressed genes were involved in T-cell activation, cell death, regulation of metabolic process, and NF-κB signaling pathway, among others (Figure 9*B*). Compared with control, the expression of pro-apoptosis genes in TCR$\gamma\delta^+$ DNT cells was increased, whereas the expression of anti-apoptosis genes in TCR$\gamma\delta^+$ DNT cells was decreased (Figure 9*C*). Meanwhile, the inflammatory response genes, such as *IL17a, IL17f, Il1b,* and *S100a8,* were also increased (Figure 9*D*). Further analysis showed that NF-κB signaling pathway related genes were up-regulated (Figure 9*E*), consistent with the results in vitro (Figure 9*F*). When NF-κB inhibitor BAY 11-7082 was added, it could partly reverse the effects of AA stimulation, which confirmed the role of NF-κB signaling pathway in AA regulating TCR$\gamma\delta^+$ DNT cells (Figure 9*G*). TFBSs in the *Il17a* promoter region were also predicted and confirmed by transcription sequencing; the promoter region of *Il17a* contains TFBSs such as vitamin D (*Vdr*), *Stat3*, *Stat4*, *Nfkb2*, androgen receptor (*Ar*), and Gata binding protein (*Gata1*) (Figure 9*H*). We further verified that *Nfkb2* was up-regulated after AA treatment and was up-regulated significantly in TCR$\gamma\delta^+$ DNT cells of NAFLD mice liver simultaneously by real-time PCR (Figure 9*I* and *J*), suggesting NF-κB signaling pathway may play a vital role in AA regulating IL17A expression.

The Numbers and Proportions of TCR$\alpha\beta^+$ DNT Cells and TCR$\gamma\delta^+$ DNT Cells in Healthy and NAFLD Patients

To validate the conclusions in mice, we analyzed the liver biopsy samples of 7 NAFLD patients and 6 healthy

Figure 8. (***See previous page***). **AA regulates TCR$\alpha\beta^+$ DNT cells function by AKT signaling pathway.** (*A*) Distributions of differential genes with up-regulated (410) and down-regulated (414) expression in TCR$\alpha\beta^+$ DNT cells with or without AA stimulation; fold change $\leq$ 0.5 or fold change $\geq$ 1.5; $P < .05$. n = 3/group. (*B* and *C*) Biological Process and KEGG pathway analysis were performed on basis of differential genes with significantly up-regulated and down-regulated expression in TCR$\alpha\beta^+$ DNT cells with or without AA stimulation. (*D* and *E*) Heatmap showing the genes related to cell death and natural killer cell mediated cytotoxicity in AA-treated TCR$\alpha\beta^+$ DNT cells and control. (*F*) Heatmap showing expression of AKT signaling pathway in AA-treated TCR$\alpha\beta^+$ DNT cells and control. (*G*) P-AKT, P50, and P-IKBα expression in TCR$\alpha\beta^+$ DNT cells after AA stimulation. n = 6 biologically independent samples per group. (*H*) Apoptosis, Bodipy, GZMB, P-AKT expression in TCR$\alpha\beta^+$ DNT cells after treating with AA and AKT agonist SC-79. n = 6 biologically independent samples per group. (*I*) The TFBSs in the upstream region (2k base pairs upstream from transcription starting site) and downstream region (100 base pairs downstream from transcription starting site) of *GzmB* were predicted. (*J*) Real-time PCR verified expression of *c-Myc* in AA-treated TCR$\alpha\beta^+$ DNT cells and control. n = 6 biologically independent samples per group. (*K*) Real-time PCR verified expression of *c-Myc* in TCR$\alpha\beta^+$ DNT cells in NAFLD and normal mice livers. n = 5 biologically independent samples per group. Two-sided P values $<.05$ were considered significant. $^{**}P < .01$; $^{*}P < .05$.

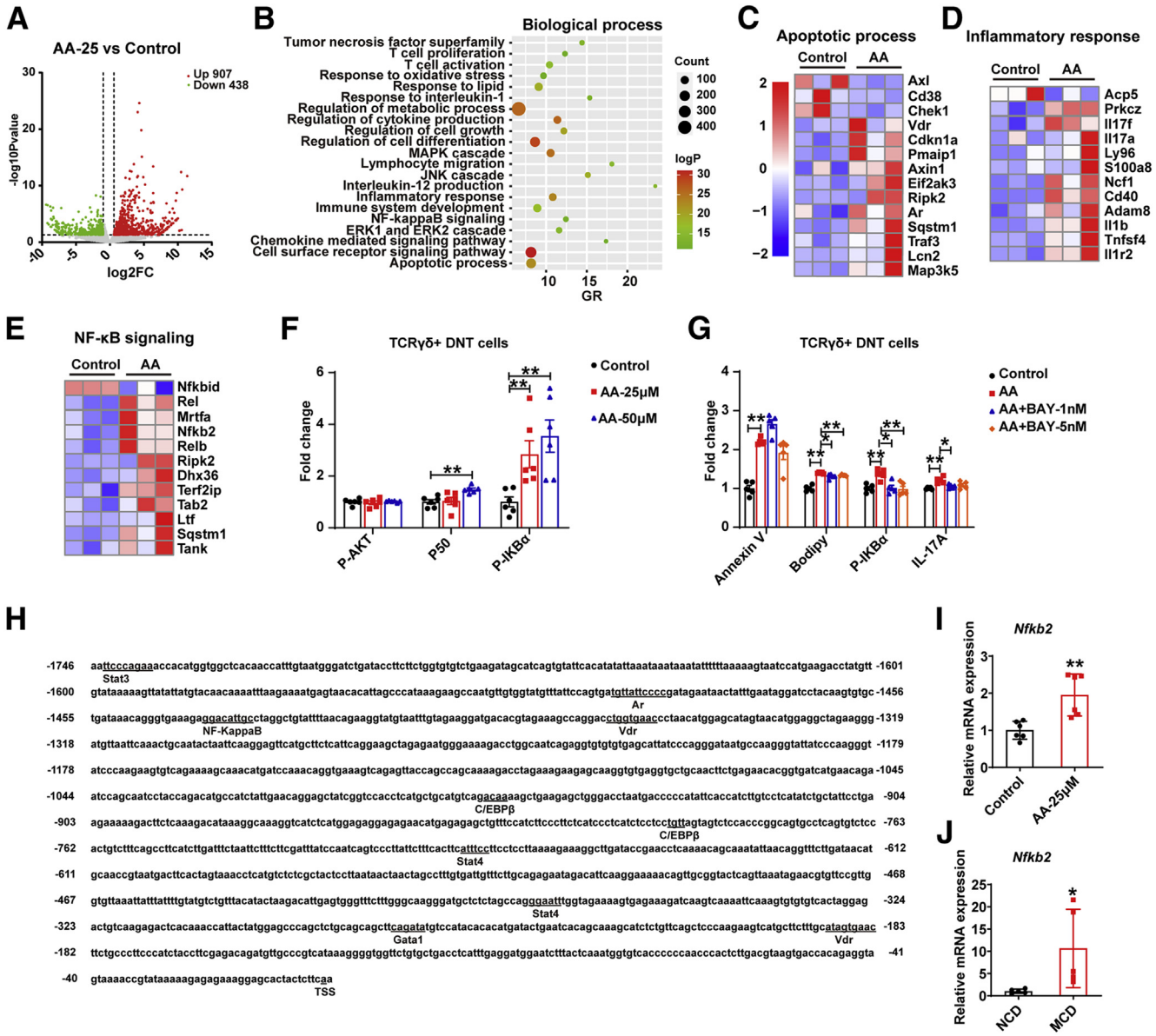

Figure 9. AA regulates TCR$\gamma\delta^+$ DNT cells function via NF-κB signaling pathway. (*A*) Distributions of differential genes with up-regulated (907) and down-regulated (438) expression in AA-treated TCR$\gamma\delta^+$ DNT cells and control; fold change $\leq$ 0.5 or fold change $\geq$ 1.5; $P < .05$. n = 3/group. (*B*) Biological Process analysis was performed on basis of differential genes with significantly up-regulated and down-regulated expression in AA-treated TCR$\gamma\delta^+$ DNT cells and control. (*C* and *D*) Heatmap showing the genes related to apoptotic process and inflammatory response in AA-treated TCR$\gamma\delta^+$ DNT cells and control. (*E*) Heatmap showing expression of NF-κB signaling pathway in AA-treated TCR$\gamma\delta^+$ DNT cells and control. (*F*) P-AKT, P50, and P-IKBα expression in TCR$\gamma\delta^+$ DNT cells after AA stimulation. n = 6 biologically independent samples per group. (*G*) Apoptosis, Bodipy, P-IKBα, and IL17A expression in TCR$\gamma\delta^+$ DNT cells after treating with AA and NF-κB inhibitor BAY 11-7082. n = 6 biologically independent samples per group. (*H*) The TFBSs in the upstream region (2k base pairs upstream from the transcription starting site) and downstream region (100 base pairs downstream from the transcription starting site) of *Il17a* were predicted. (*I*) Real-time PCR verified the expression of *Nfkb2* in AA-treated TCR$\gamma\delta^+$ DNT cells and control. n = 6 biologically independent samples per group. (*J*) Real-time PCR verified the expression of *Nfkb2* in TCR$\gamma\delta^+$ DNT cells in NAFLD and normal mice livers. n = 5 biologically independent samples per group. Two-sided *P* values <.05 were considered significant. $^{**}P < .01$; $^{*}P < .05$.

controls. CD4, CD8, CD56, TCR$\alpha\beta$, and TCR$\gamma\delta$ antibodies were used for multiplex immunofluorescence staining in liver tissues of healthy and NAFLD patients. We found higher number of TCR$\alpha\beta^+$CD4$^-$CD8$^-$CD56$^-$ cells (Figure 10*A* and *B*) and TCR$\gamma\delta^+$CD4$^-$CD8$^-$CD56$^-$ DNT cells (Figure 10*D* and *E*) per area in NAFLD patients' livers, which further confirmed the results of increased DNT cells in NAFLD mice liver (Figure 10*C* and *F*). Further analysis of the fold change

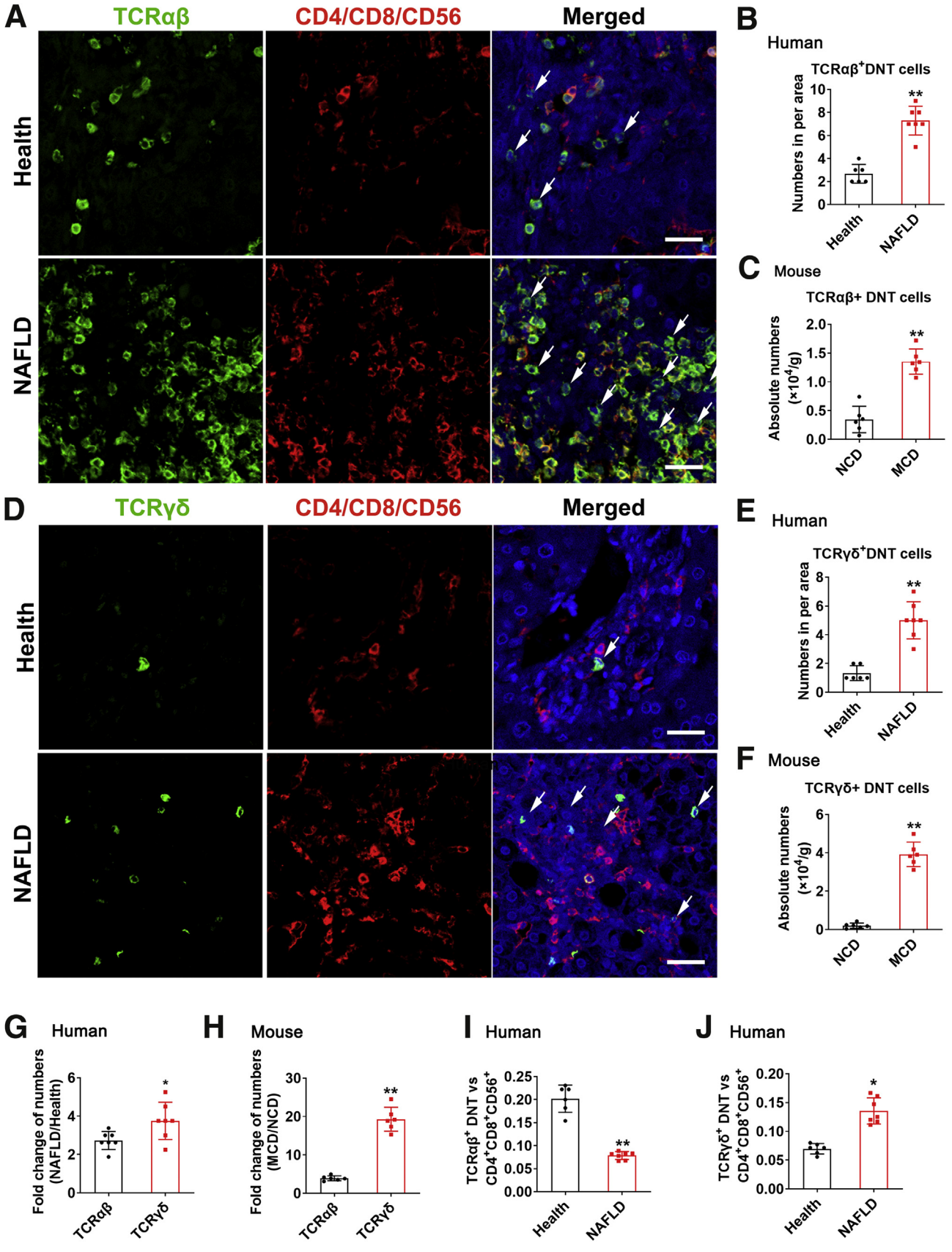
A
TCRαβ
CD4/CD8/CD56
Merged
Health
NAFLD
B
Human
TCRαβ+DNT cells
Numbers in per area
Health
NAFLD
C
Mouse
TCRαβ+ DNT cells
Absolute numbers (×10⁴/g)
NCD
MCD
D
TCRγδ
CD4/CD8/CD56
Merged
Health
NAFLD
E
Human
TCRγδ+DNT cells
Numbers in per area
Health
NAFLD
F
Mouse
TCRγδ+ DNT cells
Absolute numbers (×10⁴/g)
NCD
MCD
G
Human
Fold change of numbers (NAFLD/Health)
TCRαβ
TCRγδ
H
Mouse
Fold change of numbers (MCD/NCD)
TCRαβ
TCRγδ
I
Human
TCRαβ+ DNT vs CD4+CD8+CD56+
Health
NAFLD
J
Human
TCRγδ+ DNT vs CD4+CD8+CD56+
Health
NAFLD

of NAFLD/Health, the increase of TCR$\gamma\delta^+$ DNT cell numbers in NAFLD patients was significantly higher than that of TCR$\alpha\beta^+$ DNT cells, which was consistent with the changes in mice (Figure 10*G* and *H*).

In addition, to further detect the variation of TCR$\alpha\beta$ and TCR$\gamma\delta$ subgroups in DNT cells in human liver, we counted the ratio of TCR$\alpha\beta^+$CD4$^-$CD8$^-$CD56$^-$ T cells and TCR$\gamma\delta^+$CD4$^-$CD8$^-$CD56$^-$ with CD4$^+$CD8$^+$CD56$^+$ cells in healthy and NAFLD patients. During NAFLD development, the ratio of TCR$\alpha\beta^+$CD4$^-$CD8$^-$CD56$^-$ T cells decreased (Figure 10*I*), whereas the ratio of TCR$\gamma\delta^+$CD4$^-$CD8$^-$CD56$^-$ T cells increased (Figure 10*J*). All these results further certified the decrease of TCR$\alpha\beta^+$ DNT cell proportion and the increase of TCR$\gamma\delta^+$ DNT cell proportion in NAFLD patients, which were consistent with the conclusion in mice.

Discussion

NAFLD is now the leading cause of chronic liver disease and is increasing worldwide, but there is still a lack of satisfactory treatment. In-depth exploration of the mechanisms during the development and progression of NAFLD and NASH is important to develop strategies to address this important chronic liver disease.

Inflammation in the liver is crucial for the progression from hepatic steatosis to NASH, and infiltration of different subsets of inflammatory cells is the hallmark of steatohepatitis.[25] In this study, we found that the percentage of DNT cells in the liver was significantly higher than that in the spleen or peripheral blood, indicating the importance of DNT cells in liver immunity. However, the function of these specific T cells in liver physiology and pathology is still unclear. DNT cells play critical and diverse roles in the immune system, and they are reported to have both proinflammatory and anti-inflammatory functions. Many studies have reported that DNT cells display a unique immunoregulatory ability,[9,10,17,26] and the immune regulation of DNT cells mainly relies on the high expression of the cytotoxic molecules GZMB and perforin.[10,13,26] In this study, we found that among hepatic DNT cells, TCR$\alpha\beta^+$ DNT cells are the major source of GZMB and contribute to the maintenance of liver homeostasis. However, during NAFLD development, TCR$\alpha\beta^+$ DNT cells and their GZMB production are decreased, which results in the weakened immune regulation of TCR$\alpha\beta^+$ DNT cells and promotes NAFLD/NASH progression. Adoptive transfer of natural hepatic TCR$\alpha\beta^+$ DNT cells inhibited liver inflammation, enhanced PD-1$^+$CD122$^+$CD8-Treg cell liver infiltration, restored liver homeostasis, and significantly ameliorated NAFLD.

In this study, we also revealed that the level of IL17 secreted by hepatic TCR$\gamma\delta^+$ DNT cells was much higher than that secreted by TCR$\alpha\beta^+$ DNT cells in normal mice. During NAFLD development, IL17 production was markedly enhanced by TCR$\gamma\delta^+$ DNT cells but not TCR$\alpha\beta^+$ DNT cells, which might aggravate liver inflammation and facilitate NAFLD/NASH progression. When we eliminated TCR$\gamma\delta^+$ DNT cells, IL17 secretion by intrahepatic DNT cells was sharply decreased in the mice with NAFLD. Many studies have reported that TCR$\gamma\delta^+$ DNT cells exert significant protective effects on self-tolerance[27,28] and tumor formation[29] in mice. Human peripheral, tumor-infiltrating, small intestinal TCR$\gamma\delta^+$ DNT cells also possess immunosuppressive potential in tumors, celiac disease, and systemic lupus erythematosis.[30–34] IL17A induces Kupffer cell activation, macrophage activation, and subsequent cytokine secretion, and neutrophil accumulation plays important roles in ischemia and reperfusion injury and liver fibrosis.[35] In our study, we found that TCR$\gamma\delta^+$ DNT cell deletion decreased liver injury and M1 monocyte proportions, which indicated that these cells played important roles in the proinflammatory effects of NAFLD.

Hepatic FA metabolic disorder manifests as an imbalance between harmful FAs and beneficial FAs in NAFLD. FA synthesis, catabolism, and oxidation are pivotal for the proliferation, survival, differentiation, and function of T cells.[36,37] FA catabolism and oxidation are pivotal for the development and function of CD8$^+$ T-cell memory as well as for the differentiation of CD4$^+$ regulatory T cells.[36] Moreover, FA oxidation is an essential factor for CD8$^+$ tissue-resident memory T-cell survival in gastric adenocarcinoma.[37] In this study, we found that the harmful FA AA may be the key factor in regulating the balance of TCR$\alpha\beta^+$ DNT cells and TCR$\gamma\delta^+$ DNT cell survival and functions.

Leukotriene B4, prostaglandin E_2, and eicosanoids induced by AA are typical inflammatory mediators, and they regulate T- and B-lymphocyte functions.[38–40] Moreover, AA reduces T-cell proliferation in human peripheral blood.[41] Our results showed that AA could induce intrahepatic DNT cell apoptosis and down-regulate GZMB expression in TCR$\alpha\beta^+$ DNT cells. The AKT and NF-κB signaling pathways play a key role in regulating the immune response of immune cells, and we have also found that these signaling pathways play an important role in the regulation of TCR$\alpha\beta^+$ DNT cells by AA. We also found that in contrast to

Figure 10. (***See previous page***). **The variation tendency of DNT cells in livers of NAFLD patients was consistent with that in mice.** (*A*) Typical picture of multiplex immunofluorescence staining of human liver sections. TCR$\alpha\beta$ (*green*), CD4/CD8/CD56 (*red*). *White arrowheads* indicate DNT cells. Scale bar, 25 μm. (*B*) Number of TCR$\alpha\beta^+$ DNT cells per area in human liver. The number of DNT cells per area (150 μm $\times$ 150 μm) was counted. (*C*) Absolute number of TCR$\alpha\beta^+$DNT cells per g mouse liver. (*D*) Typical picture of multiplex immunofluorescence staining of human liver sections. TCR$\gamma\delta$ (*green*), CD4/CD8/CD56 (*red*). *White arrowheads* indicate DNT cells. Scale bar, 25 μm. (*E*) Number of TCR$\alpha\beta^+$ DNT cells per area in human liver. The number of DNT cells per area (150 μm $\times$ 150 μm) was counted. (*F*) Absolute number of TCR$\gamma\delta^+$ DNT cells per g mouse liver. (*G*) The amplitude of number variation of TCR$\gamma\delta^+$CD4$^-$CD8$^-$CD56$^-$ T cells and TCR$\alpha\beta^+$CD4$^-$CD8$^-$CD56$^-$ T cells in NAFLD/Health. (*H*) The amplitude of number variation of TCR$\alpha\beta^+$ DNT cells and TCR$\gamma\delta^+$ DNT cells in MCD/NCD. (*I*) Ratio of TCR$\alpha\beta^+$DNT cells with CD4$^+$CD8$^+$CD56$^+$ cells (0.02 cm^2 per area). (*J*) Ratio of TCR$\gamma\delta^+$ DNT cells with CD4$^+$CD8$^+$CD56$^+$ cells (0.02 cm^2 per area). Two-sided *P* values $<$.05 were considered significant. $^{**}P < .01$; $^{*}P < .05$.

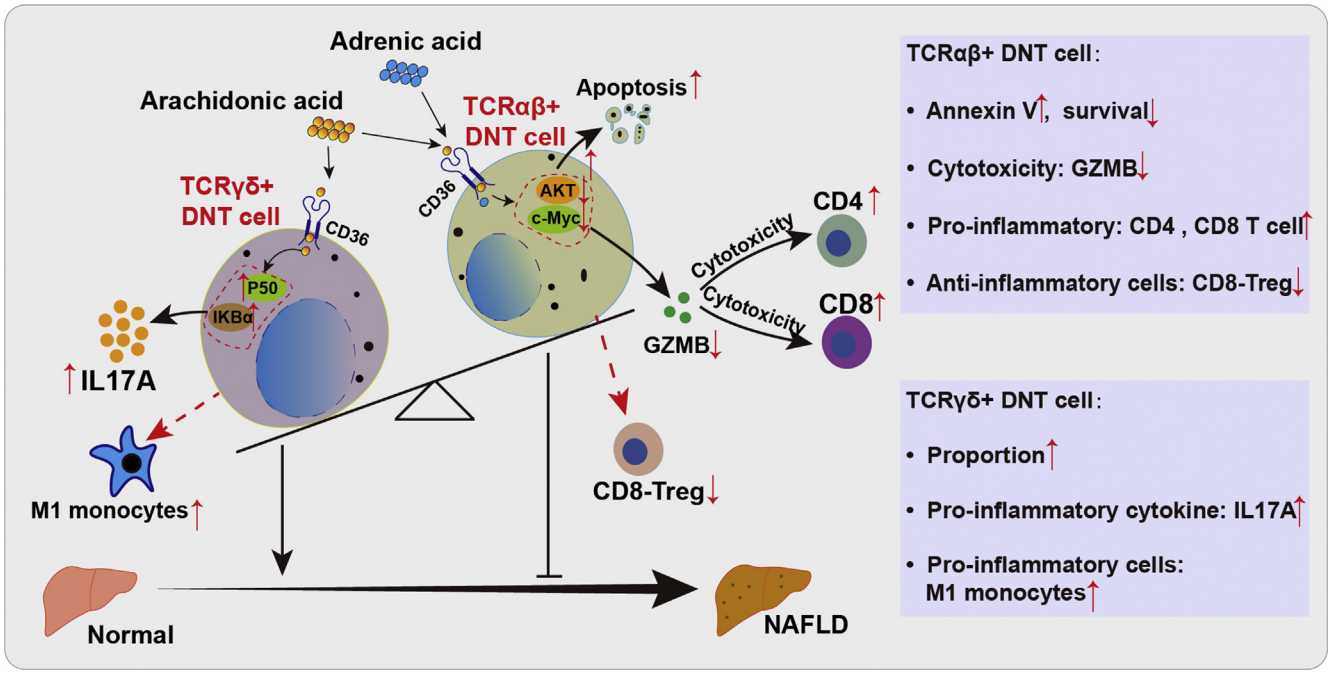

Figure 11. Intrinsic mechanisms of AA and ADA regulation on TCR$\alpha\beta+$ and TCR$\gamma\delta+$ DNT cells during NAFLD development. AA and ADA induced apoptosis of TCR$\alpha\beta^+$ DNT cells and decreased their immunosuppressive function, which were mainly associated with the AKT signaling pathway during NAFLD development. AA also facilitated IL17A secretion by TCR$\gamma\delta^+$ DNT cells, which was mainly associated with the NF-κB signaling pathway.

the effect on TCR$\alpha\beta^+$ DNT cells, AA promoted the secretion of IL17A by TCR$\gamma\delta^+$ DNT cells, suggesting that it also promoted the inflammatory response and that the NF-κB signaling pathway may be involved. The discrepant effects of FAs on TCR$\alpha\beta^+$ and TCR$\gamma\delta^+$ DNT cells need in-depth exploration in the future.

In conclusion, our data revealed that AA and ADA induced apoptosis of TCR$\alpha\beta^+$ DNT cells and decreased their immunosuppressive function, which was mainly associated with the AKT signaling pathway during NAFLD development. AA also facilitated IL17A secretion by TCR$\gamma\delta^+$ DNT cells, which was mainly associated with the NF-κB signaling pathway (Figure 11). Exploring the different functions of TCR subtypes would help elucidate the role of DNT cells in the progression of NAFLD, and potentially controlling the different DNT subtypes will contribute to NAFLD therapy.

Methods

Animals and Treatment

Eight-week-old weight-matched male C57BL/6 mice and CD45.1 congenic C57BL/6 mice were purchased from The Jackson Laboratory (Bar Harbor, ME). MCD has short modeling duration, low cost, and easy acquisition, which can effectively induce steatosis and steatohepatitis, and the lipid distribution in liver can simulate human NAFLD well.[42–44] One of the most important disadvantages of the MCD model is that the extrahepatic metabolic performance differs from that of the vast majority of human NAFLD patients, with this model displaying significant loss weight gain and decreased blood glucose levels.[44] In addition, CDHFD-fed mice also developed well to mimic human NAFLD and fibrosis disease.[44] Because of its long duration, it has a high chance of progressing to liver cancer.[45] Thus, we mainly used these 2 diets to induce NAFLD models. After being allowed to adapt for 5 days, the C57BL/6 mice were fed either a NCD or a MCD (10401; Beijing HFK Bioscience, Beijing, China) for 5 weeks or a CDHFD for 18 weeks. The mice were housed in a pathogen-free, comfortable temperature environment with a 12-hour light/dark cycle. All animal studies were performed in compliance with the ethical guidelines for animal studies and approved by the animal ethics committee of Beijing Friendship Hospital, Capital Medical University.

Enzyme-Linked Immunosorbent Assay and H&E, Oil Red O, and Immunohistochemistry Staining of α-SMA

Serum AST and ALT enzyme-linked immunosorbent assay kits were obtained from Jiancheng (Nanjing, China). All experiments followed the manufacturer's instructions. The left lobes of livers were fixed with 4% paraformaldehyde and then stained with H&E, Oil Red O staining, and immunohistochemistry for α-SMA by Servicebio Technology (Wuhan, China).

Flow Cytometry

The isolation and detection of hepatic immune cells were conducted as previously described.[46] Immune cells were harvested, and the expression of various cell surface, intracellular, and intranuclear markers was determined

Table 1. Various Cell Surface, Intracellular, and Intranuclear Markers in This Study

Manufacturer	Mouse antibody	Clone/catalog number
BioLegend (USA)	CD45 (PE/Cyanine7)	S18009F
	CD45 (FITC)	QA17A26
	CD45 (BV510)	30-F11
	CD45(APC/Cyanine7)	30-F11
	CD45 (BV605)	30-F11
	CD3 (Percp/Cyanine5.5)	17A2
	CD3 (APC)	17A2
	CD3 (PE/Cyanine7)	17A2
	CD3 (PE)	17A2
	CD3 (BV785)	17A2
	NK1.1 (PE)	S17016D
	NK1.1(FITC)	S17016D
	NK1.1 (BV421)	PK136
	NK1.1 (BV605)	PK136
	CD4 (PE)	GK1.5
	CD4 (Percp)	GK1.5
	CD4 (PE/Cyanine7)	GK1.5
	CD4 (BV785)	GK1.5
	CD4 (Pacific Blue)	GK1.5
	CD4 (FITC)	GK1.5
	CD4 (BV650)	GK1.5
	CD8a (APC)	53-6.7
	CD8a (PE)	53-6.7
	CD8a (APC/Cyanine7)	53-6.7
	CD8a (FITC)	53-6.7
	Annexin V (APC)	640941
	Annexin V (PE)	640934
	Annexin V (FITC)	640906
	7-AAD (Percp/ Cyanine5.5)	420404
	Ki67(FITC)	16A8
	TCRβ (FITC)	H57-597
	TCRβ (PE/Cyanine7)	H57-597
	TCRβ (Percp/Cyanine5.5)	H57-597
	TCR$\gamma\delta$ (PE)	UC7-13D5
	TCR$\gamma\delta$ (APC)	GL3
	CD36 (APC)	HM36
	Ly6G (APC/Cyanine7)	1A8
	CD11b (BV421)	M1/70
	F4/80 (PE)	BM8
	CD11c (FITC)	N418
	CD206 (APC)	C068C2
	IL17A (PE)	TC11-18H10.1
	GZMB (FITC)	GB11
	GZMB (PE)	QA16A02
	GZMB (APC)	QA16A02
	IFNγ (BV711)	XMG1.2
eBioscience	NKG2D (PE)	A10
	CD122 (PE)	TM-b1(TM-beta1)
	P-AKT(APC)	SDRNR
Abcam	NFκB P105/P50	ab19285
	P-IKB αlphα	ab32518
	Goat pAb to Rb IgG (Alexa Fluor 488)	ab150077
Invitrogen	BODIPYTM 493/503	D3922

Table 2. Primers in This Study

		Sequence
GAPDH	Forward Primer	AAGGTCATCCCAGAGCTGAA
	Reverse Primer	CTGCTTCACCACCTTCTTGA
Bik	Forward Primer	CTGCGTCAACACTGCCAGATA
	Reverse Primer	CTTGTCCTTAATGCGGCTCAG
Arrb1	Forward Primer	AAGGGACACGAGTGTTCAAGA
	Reverse Primer	CCCGCTTTCCCAGGTAGAC
Atf6	Forward Primer	TGGAGCAGGATGTCCCGTT
	Reverse Primer	CTGTGGAAAGATGTGAGGACTC
Rarg	Forward Primer	ATGTACGACTGCATGGAATCG
	Reverse Primer	CCAGTGGCTCTGCGTAGTAA
Top2a	Forward Primer	CAACTGGAACATATACTGCTCCG
	Reverse Primer	GGGTCCCTTTGTTTGTTATCAGC
Ccna2	Forward Primer	GCCTTCACCATTCATGTGGAT
	Reverse Primer	TTGCTCCGGGTAAAGAGACAG

(Table 1). A FACS Aria II flow cytometer (BD Biosciences, San Jose, CA) was applied to measure all samples, and FlowJo software version V10 data were used to analyze the data.

Transcriptome Sequencing Analysis

Intrahepatic DNT cells from the NCD- and MCD-fed mice were sorted by a FACS Aria II flow cytometer, and total RNA was isolated. Transcriptome sequencing libraries were sequenced on an Illumina HiSeq 2000 platform (Illumina, San Diego, CA) following the manufacturer's recommendations. After the measurement of fragments per kilobase per million mapped reads value, we performed a differential expression analysis of the transcripts with P value $<.05$ and fold change ≤ 0.5 or fold change ≥ 1.5 between the NCD- and MCD-fed mice, and these transcripts were submitted to GO and KEGG enrichment analysis, which uses unbiased methods to assess pathway enrichment.

Quantitative Real-Time Reverse Transcription–PCR

Total RNA of primary DNT cells from NCD- or MCD-fed mouse livers was isolated using TRIzol Reagent (T9424-200ML; Sigma-Aldrich, St Louis, MO), and first strand cDNA was synthesized using PrimeScript RT Master Mix (RR037A; TaKaRa, Japan) according to the manufacturer's instructions. The cDNA was subjected to PCR cycles with SYBR Green quantitative PCR reagent (11202ES08; Yeasen, Shanghai, China), and assays were conducted using the ABI 7500 sequence detection system (Applied Biosystems, Waltham, MA). The primers are presented in Table 2.

TCR$\gamma\delta^+$ DNT Depletion Assay

Injections with 400 μg anti-mouse TCRγ/δ (BE0070-25MG; Bio X Cell, Lebanon, NH) were administered on day −2, and administration of 200 μg InVivoMab anti-mouse TCRγ/δ was repeated on days −1, 3, 6, 10, 13, 17, 20, 24, 27, 31, 34, 38, and 41. Phosphate-buffered saline served as the control group. On day 43, mice were killed for the study of progressive NAFLD as described above.

TCR$\alpha\beta^+$ DNT Cells Adoptive Transfer Administration in Vivo

TCR$\alpha\beta^+$ DNT cells were isolated from C57BL/6 mouse liver by a fluorescence-activated cell sorter (FACS Aria II; BD Biosciences). In the MCD-fed NAFLD model, the C57BL/6 mice received an adoptive transfer of 3×10^6 CD45.1-positive DNT (purity $> 97\%$) and were fed the MCD for 5 weeks; then liver inflammation and lymphocytes proportion were detected as described above.

Metabonomics and FA Stimulation Assay

A liver sample (50 mg) from the NCD- and MCD-fed mice was subjected to identification and quantification of the 65 FFAs using a Q300 Metabolite Array Kit (Metabo-Profile, Shanghai, China). CD3$^+$ T cells were enriched from C57BL/6 mouse spleens by a mouse CD3$^+$ T-cell enrichment column (R&D Systems, Minneapolis, MN). Isolated CD3$^+$ T cells were cultured in wells precoated with the anti-CD3 monoclonal antibody (5 μg/mL; BD Biosciences) and the anti-CD28 monoclonal antibody (2 μg/mL; BD Biosciences) and then with 25 or 50 μmol/L ADA, AA (MCE, Monmouth Junction, NJ), or dimethyl sulfoxide at 37°C with 5% CO_2 for 48 hours, and 25 μmol/L ADA group was sent to transcriptome sequencing after extracting RNA by RNasey Plus Micro Kit according to instructions (Qiagen, Hilden. Germany). Then, flow cytometry was conducted to assess apoptosis and cell surface markers of DNT cells. One μmol/L, 5 μmol/L AKT activator SC-79 (MCE) or 1 nmol/L, 5 nmol/L NF-κB signaling pathway inhibitor BAY 11-7082 (MCE) were used to interrupt effect induced by AA in TCR$\alpha\beta^+$ DNT cells or TCR$\gamma\delta^+$ DNT cells for 48 hours.

Table 2. Continued

		Sequence
Ppp2ca	Forward Primer	ATGGACGAGAAGTTGTTCACC
	Reverse Primer	CAGTGACTGGACATCGAACCT
Ect2	Forward Primer	AACTTGTGCTTGGCGTCTACT
	Reverse Primer	TTCCTCCGATTTTCCAGGACA
Dusp6	Forward Primer	ATAGATACGCTCAGACCCGTG
	Reverse Primer	ATCAGCAGAAGCCGTTCGTT
Mcl1	Forward Primer	AAAGGCGGCTGCATAAGTC
	Reverse Primer	TGGCGGTATAGGTCGTCCTC
Ncr1	Forward Primer	ATGCTGCCAACACTCACTG
	Reverse Primer	GATGTTCACCGAGTTTCCATTTG
Klrb1c	Forward Primer	ATGGACACAGCAAGTATCTACCT
	Reverse Primer	AGCTCTCAGGAGTCACTTTATCT
Klrg1	Forward Primer	TCTCATCCCTTCCTCTGC
	Reverse Primer	TTGCGTCTTTCTGTCTTGT
Havcr2	Forward Primer	ACTGGTGACCCTCCATAATAACA
	Reverse Primer	GCAGTTCTGATCGTTTCTCCA
Fyn	Forward Primer	TCAACACGGGGAGTAACCC
	Reverse Primer	CGAGCTTTGTCCTGCAACT
Klra1	Forward Primer	GTTCCTTCAGACGTTTGCTGG
	Reverse Primer	ATTGTCAACCCATGACCAATCTT
IL1R1	Forward Primer	GTGCTACTGGGGCTCATTTGT
	Reverse Primer	GGAGTAAGAGGACACTTGCGAAT
IL2Ra	Forward Primer	AACCATAGTACCCAGTTGTCGG
	Reverse Primer	TCCTAAGCAACGCATATAGACCA
Ahr	Forward Primer	ACATACGCCGGTAGGAAGAGA
	Reverse Primer	GGTCCAGCTCTGTATTGAGGC
Rorc	Forward Primer	AGGAGAGCGTTCCAAGACCA
	Reverse Primer	AGTTTCCGCTTCATGCTACTG
Il17a	Forward Primer	GCTCCAGAAGGCCCTCAGACT
	Reverse Primer	CCAGCTTTCCCTCCGCATTGA
Il17f	Forward Primer	TGCTACTGTTGATGTTGGGAC
	Reverse Primer	AATGCCCTGGTTTTGGTTGAA
Ifngr2	Forward Primer	TCCTCGCCAGACTCGTTTTC
	Reverse Primer	GTCTTGGGTCATTGCTGGAAG
IL21R	Forward Primer	GGCTGCCTTACTCCTGCTG
	Reverse Primer	TCATCTTGCCAGGTGAGACTG
IL-23R	Forward Primer	TTCAGATGGGCATGAATGTTTCT
	Reverse Primer	CCAAATCCGAGCTGTTGTTCTAT
CD36	Forward Primer	ATGGGCTGTGATCGGAACTG
	Reverse Primer	GTCTTCCCAATAAGCATGTCTCC
Pdcd1	Forward Primer	TTCACCTGCAGCTTGTCCAA
	Reverse Primer	TGGGCAGCTGTATGATCTGG
Fasl	Forward Primer	TGAATTACCCATGTCCCCAG
	Reverse Primer	AAACTGACCCTGGAGGAGCC
Perforin	Forward Primer	CTGCCACTCGGTCAGAATG
	Reverse Primer	CGGAGGGTAGTCACATCCAT
Granzyme B	Forward Primer	ATCCTGCTCTGATTACCCATCGT
	Reverse Primer	ATGGACATGAAGCCAGTCTTTGC
IFN-γ	Forward Primer	GGCCATCAGCAACAACATAAGCGT
	Reverse Primer	TGGGTTGTTGACCTCAAACTTGGC

Table 2. Continued

		Sequence
Klrk1	Forward Primer	ACTCAGAGATGAGCAAATGCC
	Reverse Primer	CAGGTTGACTGGTAGTTAGTGC
Klra7	Forward Primer	GCAGAAACTAGTGAGGACTGAG
	Reverse Primer	TTACCAGGAGAAGGAAACAGAAG
Klrd1	Forward Primer	TCTAGGATCACTCGGTGGAGA
	Reverse Primer	CACTTGTCCAGGCAAACACAG
Klrc1	Forward Primer	AGAAACTCATTGCTGGTA
	Reverse Primer	CCTTTGCTTCGGTAT
Ifngr1	Forward Primer	TTGACGAGCACTGAGGA
	Reverse Primer	AGGAACCCGAATACACC
IL-4	Forward Primer	GTCATCCTGCTCTTCTTT
	Reverse Primer	ATGGCGTCCCTTCTC
Jak2	Forward Primer	CCACGGCCCAATATCAATG
	Reverse Primer	CCCGCCTTCTTTAGTTTGCTA
Cxcl16	Forward Primer	CCTTGTCTCTTGCGTTCTTCC
	Reverse Primer	TCCAAAGTACCCTGCGGTATC
c-Myc	Forward Primer	TCTCCACTCACCAGCACAACTACG
	Reverse Primer	ATCTGCTTCAGGACCCT
Nfkb2	Forward Primer	GGCCGGAAGACCTATCCTACT
	Reverse Primer	CTACAGACACAGCGCACACT

Clinical Study

Seven patients diagnosed with NAFLD were confirmed by liver biopsy specimen at Capital Medical University, Beijing Friendship Hospital. NAFLD patients were consuming less than 10 g alcohol/day for women and 20 g alcohol/day for men, and other causes of steatosis or chronic liver disease were excluded. Healthy liver tissues were obtained from 6 donors whose livers were subsequently used for liver transplantation. Written informed consent was obtained from all patients before their enrollment, and the study protocol was approved by the Human Institutional Review Board of Beijing Friendship Hospital (No. 2017-P2-131-03).

Human liver tissues were fixed in 4% paraformaldehyde for 48 hours and then embedded in paraffin, sectioned at 5 μm for immunofluorescence staining. After deparaffinization and rehydration, we performed antigen unmasking using heat treatment with citrate solution, followed by incubating with 10% H_2O_2 to neutralize endogenous peroxidase activity. We blocked nonspecific binding sites with goat serum for 1 hour at 37°C. Then the sections were incubated overnight at 4°C with the primary antibodies against TCRα (Santa Cruz Biotechnology, Dallas, TX; sc-515719, 1:50), TCRδ (Santa Cruz Biotechnology; sc-100289, 1:50), CD4 (Beijing Zhongshan Golden Bridge Biotechnology Co; TA500481, 1:50), CD8 (Cell Signaling Technology, Danvers, MA; 70306s, 1:50), and CD56 (Cell Signaling Technology; 99746s, 1:50). The secondary antibodies (Beijing Zhongshan Golden Bridge Biotechnology Co) were added and then incubated at room temperature for 1 hour before TSA reaction. The sections were observed by microscopy (FV1000; Olympus, Tokyo, Japan).

Statistical Analysis

Statistical analysis was performed by using SPSS Statistics (IBM SPSS Statistics for Windows, Version 22.0; Armonk, NY) and Prism 8.0 software (GraphPad Software, San Diego, CA). Values are expressed as the mean ± standard error of the mean. The normal distribution of variables was tested with the Shapiro–Wilk test. Differences between 2 groups were compared by *t* tests for normal variables and Kruskal–Wallis tests for non-normal variables. One-way analysis of variance with post hoc test for normal variables and Kruskal–Wallis tests for non-normal variables were used in multiple comparisons. Two-sided *P* values $<.05$ were considered significant.

References

1. Younossi Z, Anstee QM, Marietti M, Hardy T, Henry L, Eslam M, George J, Bugianesi E. Global burden of NAFLD and NASH: trends, predictions, risk factors and prevention. Nat Rev Gastroenterol Hepatol 2018; 15:11–20.
2. Petroni ML, Brodosi L, Bugianesi E, Marchesini G. Management of non-alcoholic fatty liver disease. BMJ 2021;372:m4747.
3. Sheka AC, Adeyi O, Thompson J, Hameed B, Crawford PA, Ikramuddin S. Nonalcoholic steatohepatitis: a review. JAMA 2020;323:1175–1183.
4. Cai J, Zhang XJ, Li H. The role of innate immune cells in nonalcoholic steatohepatitis. Hepatology 2019; 70:1026–1037.
5. Sutti S, Albano E. Adaptive immunity: an emerging player in the progression of NAFLD. Nat Rev Gastroenterol Hepatol 2020;17:81–92.

6. Brandt D, Hedrich CM. TCRalphabeta(+)CD3(+)CD4(-)CD8(-) (double negative) T cells in autoimmunity. Autoimmun Rev 2018;17:422–430.
7. Juvet SC, Zhang L. Double negative regulatory T cells in transplantation and autoimmunity: recent progress and future directions. J Mol Cell Biol 2012;4:48–58.
8. Hillhouse EE, Lesage S. A comprehensive review of the phenotype and function of antigen-specific immunoregulatory double negative T cells. J Autoimmun 2013;40:58–65.
9. Fischer K, Voelkl S, Heymann J, Przybylski GK, Mondal K, Laumer M, Kunz-Schughart L, Schmidt CA, Andreesen R, Mackensen A. Isolation and characterization of human antigen-specific TCR alpha beta+ CD4(-)CD8- double-negative regulatory T cells. Blood 2005;105:2828–2835.
10. Zhang D, Yang W, Degauque N, Tian Y, Mikita A, Zheng XX. New differentiation pathway for double-negative regulatory T cells that regulates the magnitude of immune responses. Blood 2007;109:4071–4079.
11. Zhang D, Zhang W, Ng TW, Wang Y, Liu Q, Gorantla V, Lakkis F, Zheng XX. Adoptive cell therapy using antigen-specific CD4(-)CD8(-)T regulatory cells to prevent autoimmune diabetes and promote islet allograft survival in NOD mice. Diabetologia 2011;54:2082–2092.
12. Maccari ME, Fuchs S, Kury P, Andrieux G, Volkl S, Bengsch B, Lorenz MR, Heeg M, Rohr J, Jagle S, Castro CN, Gross M, Warthorst U, Konig C, Fuchs I, Speckmann C, Thalhammer J, Kapp FG, Seidel MG, Duckers G, Schonberger S, Schutz C, Fuhrer M, Kobbe R, Holzinger D, Klemann C, Smisek P, Owens S, Horneff G, Kolb R, Naumann-Bartsch N, Miano M, Staniek J, Rizzi M, Kalina T, Schneider P, Erxleben A, Backofen R, Ekici A, Niemeyer CM, Warnatz K, Grimbacher B, Eibel H, Mackensen A, Frei AP, Schwarz K, Boerries M, Ehl S, Rensing-Ehl A. A distinct CD38+CD45RA+ population of CD4+, CD8+, and double-negative T cells is controlled by FAS. J Exp Med 2021:218.
13. Zhang ZX, Ma Y, Wang H, Arp J, Jiang J, Huang X, He KM, Garcia B, Madrenas J, Zhong R. Double-negative T cells, activated by xenoantigen, lyse autologous B and T cells using a perforin/granzyme-dependent, Fas-Fas ligand-independent pathway. J Immunol 2006;177:6920–6929.
14. Li W, Tian Y, Li Z, Gao J, Shi W, Zhu J, Zhang D. Ex vivo converted double negative T cells suppress activated B cells. Int Immunopharmacol 2014;20:164–169.
15. Gao JF, McIntyre MS, Juvet SC, Diao J, Li X, Vanama RB, Mak TW, Cattral MS, Zhang L. Regulation of antigen-expressing dendritic cells by double negative regulatory T cells. Eur J Immunol 2011;41:2699–2708.
16. Su Y, Huang X, Wang S, Min WP, Yin Z, Jevnikar AM, Zhang ZX. Double negative Treg cells promote non-myeloablative bone marrow chimerism by inducing T-cell clonal deletion and suppressing NK cell function. Eur J Immunol 2012;42:1216–1225.
17. Zhang ZX, Yang L, Young KJ, DuTemple B, Zhang L. Identification of a previously unknown antigen-specific regulatory T cell and its mechanism of suppression. Nat Med 2000;6:782–789.
18. Voelkl S, Gary R, Mackensen A. Characterization of the immunoregulatory function of human TCR-alphabeta+ CD4- CD8- double-negative T cells. Eur J Immunol 2011;41:739–748.
19. Crispin JC, Oukka M, Bayliss G, Cohen RA, Van Beek CA, Stillman IE, Kyttaris VC, Juang YT, Tsokos GC. Expanded double negative T cells in patients with systemic lupus erythematosus produce IL-17 and infiltrate the kidneys. J Immunol 2008;181:8761–8766.
20. Alunno A, Bistoni O, Bartoloni Bocci E, Caterbi S, Bigerna B, Pucciarini A, Tabarrini A, Mannucci R, Beghelli D, Falini B, Gerli R. IL-17-producing double-negative T cells are expanded in the peripheral blood, infiltrate the salivary gland and are partially resistant to corticosteroid therapy in patients with Sjogren's syndrome. Reumatismo 2013;65:192–198.
21. Li H, Adamopoulos IE, Moulton VR, Stillman IE, Herbert Z, Moon JJ, Sharabi A, Krishfield S, Tsokos MG, Tsokos GC. Systemic lupus erythematosus favors the generation of IL-17 producing double negative T cells. Nat Commun 2020;11:2859.
22. Sun G, Zhao X, Li M, Zhang C, Jin H, Li C, Liu L, Wang Y, Shi W, Tian D, Xu H, Tian Y, Wu Y, Liu K, Zhang Z, Zhang D. CD4 derived double negative T cells prevent the development and progression of nonalcoholic steatohepatitis. Nat Commun 2021;12:650.
23. Wang J, Wang H, Peters M, Ding N, Ribback S, Utpatel K, Cigliano A, Dombrowski F, Xu M, Chen X, Song X, Che L, Evert M, Cossu A, Gordan J, Zeng Y, Chen X, Calvisi DF. Loss of Fbxw7 synergizes with activated Akt signaling to promote c-Myc dependent cholangiocarcinogenesis. J Hepatol 2019;71:742–752.
24. Zhang F, Li K, Yao X, Wang H, Li W, Wu J, Li M, Zhou R, Xu L, Zhao L. A miR-567-PIK3AP1-PI3K/AKT-c-Myc feedback loop regulates tumour growth and chemoresistance in gastric cancer. EBioMedicine 2019;44:311–321.
25. Tilg H, Moschen AR. Evolution of inflammation in nonalcoholic fatty liver disease: the multiple parallel hits hypothesis. Hepatology 2010;52:1836–1846.
26. Zhao X, Sun G, Sun X, Tian D, Liu K, Liu T, Cong M, Xu H, Li X, Shi W, Tian Y, Yao J, Guo H, Zhang D. A novel differentiation pathway from CD4(+) T cells to CD4(-) T cells for maintaining immune system homeostasis. Cell Death Dis 2016;7:e2193.
27. Locke NR, Stankovic S, Funda DP, Harrison LC. TCR gamma delta intraepithelial lymphocytes are required for self-tolerance. J Immunol 2006;176:6553–6559.
28. Ashour HM, Niederkorn JY. Gammadelta T cells promote anterior chamber-associated immune deviation and immune privilege through their production of IL-10. J Immunol 2006;177:8331–8337.
29. Seo N, Tokura Y, Takigawa M, Egawa K. Depletion of IL-10- and TGF-beta-producing regulatory gamma delta T cells by administering a daunomycin-conjugated specific monoclonal antibody in early tumor lesions augments the activity of CTLs and NK cells. J Immunol 1999;163:242–249.

30. Kuhl AA, Pawlowski NN, Grollich K, Blessenohl M, Westermann J, Zeitz M, Loddenkemper C, Hoffmann JC. Human peripheral gammadelta T cells possess regulatory potential. Immunology 2009;128:580–588.
31. Peng G, Wang HY, Peng W, Kiniwa Y, Seo KH, Wang RF. Tumor-infiltrating gammadelta T cells suppress T and dendritic cell function via mechanisms controlled by a unique toll-like receptor signaling pathway. Immunity 2007;27:334–248.
32. Bhagat G, Naiyer AJ, Shah JG, Harper J, Jabri B, Wang TC, Green PH, Manavalan JS. Small intestinal CD8+TCRgammadelta+NKG2A+ intraepithelial lymphocytes have attributes of regulatory cells in patients with celiac disease. J Clin Invest 2008;118:281–293.
33. Li X, Kang N, Zhang X, Dong X, Wei W, Cui L, Ba D, He W. Generation of human regulatory gammadelta T cells by TCRgammadelta stimulation in the presence of TGF-beta and their involvement in the pathogenesis of systemic lupus erythematosus. J Immunol 2011; 186:6693–6700.
34. Ye J, Ma C, Hsueh EC, Eickhoff CS, Zhang Y, Varvares MA, Hoft DF, Peng G. Tumor-derived gammadelta regulatory T cells suppress innate and adaptive immunity through the induction of immunosenescence. J Immunol 2013;190:2403–2414.
35. Giles DA, Moreno-Fernandez ME, Divanovic S. IL-17 axis driven inflammation in non-alcoholic fatty liver disease progression. Curr Drug Targets 2015;16:1315–1323.
36. Lochner M, Berod L, Sparwasser T. Fatty acid metabolism in the regulation of T cell function. Trends Immunol 2015;36:81–91.
37. Lin R, Zhang H, Yuan Y, He Q, Zhou J, Li S, Sun Y, Li DY, Qiu HB, Wang W, Zhuang Z, Chen B, Huang Y, Liu C, Wang Y, Cai S, Ke Z, He W. Fatty acid oxidation controls CD8(+) tissue-resident memory T-cell survival in gastric adenocarcinoma. Cancer Immunol Res 2020;8:479–492.
38. Calder PC. Immunomodulation by omega-3 fatty acids. Prostaglandins Leukot Essent Fatty Acids 2007; 77:327–335.
39. Valitutti S, Castellino F, Aiello FB, Ricci R, Patrignani P, Musiani P. The role of arachidonic acid metabolite PGE2 on T cell proliferative response. J Clin Lab Immunol 1989; 29:167–173.
40. Kawahara K, Hohjoh H, Inazumi T, Tsuchiya S, Sugimoto Y. Prostaglandin E2-induced inflammation: relevance of prostaglandin E receptors. Biochim Biophys Acta 2015;1851:414–421.
41. Zurier RB, Rossetti RG, Seiler CM, Laposata M. Human peripheral blood T lymphocyte proliferation after activation of the T cell receptor: effects of unsaturated fatty acids. Prostaglandins Leukot Essent Fatty Acids 1999; 60:371–375.
42. Marcolin E, Forgiarini LF, Tieppo J, Dias AS, Freitas LA, Marroni NP. Methionine- and choline-deficient diet induces hepatic changes characteristic of non-alcoholic steatohepatitis. Arq Gastroenterol 2011;48:72–79.
43. Haberl EM, Pohl R, Rein-Fischboeck L, Horing M, Krautbauer S, Liebisch G, Buechler C. Hepatic lipid profile in mice fed a choline-deficient, low-methionine diet resembles human non-alcoholic fatty liver disease. Lipids Health Dis 2020;19:250.
44. Jahn D, Kircher S, Hermanns HM, Geier A. Animal models of NAFLD from a hepatologist's point of view. Biochim Biophys Acta Mol Basis Dis 2019; 1865:943–953.
45. Marquez-Quiroga LV, Arellanes-Robledo J, Vasquez-Garzon VR, Villa-Trevino S, Muriel P. Models of nonalcoholic steatohepatitis potentiated by chemical inducers leading to hepatocellular carcinoma. Biochem Pharmacol 2022;195:114845.
46. Sun G, Jin H, Zhang C, Meng H, Zhao X, Wei D, Ou X, Wang Q, Li S, Wang T, Sun X, Shi W, Tian D, Liu K, Xu H, Tian Y, Li X, Guo W, Jia J, Zhang Z, Zhang D. OX40 regulates both innate and adaptive immunity and promotes nonalcoholic steatohepatitis. Cell Rep 2018; 25:3786–3799 e4.

Received August 11, 2021. Accepted February 24, 2022.

Correspondence
Address correspondence to: Guangyong Sun, PhD, Capital Medical University Affiliated Beijing Friendship Hospital, Yongan Street 95#, Xicheng District, Beijing 100050, China. e-mail: sungy@ccmu.edu.cn; fax: (8610)63139421; or Dong Zhang, PhD, Capital Medical University Affiliated Beijing Friendship Hospital, Yongan Street 95#, Xicheng District, Beijing 100050, China. e-mail: zhangd@ccmu.edu.cn.

CRediT Authorship Contributions
Changying Li (Data curation: Lead; Formal analysis: Lead; Investigation: Lead; Methodology: Lead; Project administration: Lead; Resources: Equal; Software: Lead; Validation: Lead; Visualization: Lead; Writing – original draft: Lead; Writing – review & editing: Supporting)
Xiaonan Du (Data curation: Equal; Formal analysis: Equal; Investigation: Equal; Methodology: Equal)
Zongshan Shen (Data curation: Supporting; Formal analysis: Supporting; Methodology: Supporting)
Yunxiong Wei (Data curation: Supporting; Investigation: Supporting; Resources: Supporting; Supervision: Supporting)
Yaning Wang (Data curation: Supporting)
Xiaotong Han (Data curation: Supporting)
Hua Jin (Data curation: Supporting)
Chunpan Zhang (Data curation: Supporting)
Mengyi Li (Methodology: Supporting; Resources: Supporting; Supervision: Supporting)
Zhongtao Zhang (Project administration: Supporting; Supervision: Supporting)
Songlin Wang (Supervision: Supporting)
Dong Zhang (Funding acquisition: Equal; Methodology: Supporting; Project administration: Lead; Resources: Lead; Writing – review & editing: Equal)
Guangyong Sun (Funding acquisition: Lead; Resources: Equal; Supervision: Lead; Writing – review & editing: Lead)

Conflicts of interest
The authors disclose no conflicts.

Funding
Supported by grants from the National Natural Science Foundation of China (No. 81870399, 81970503, 82001694 and 82070580), the Beijing Natural Science Foundation (7192046), and Youth Beijing Scholar (No. 035).